PLOS COMPUTATIONAL BIOLOGY

RESEARCH ARTICLE

Toward an optimal contraception dosing strategy

Brenda Lyn A. Gavina[1,2], Aurelio A. de los Reyes V[1,3]*, Mette S. Olufsen[4], Suzanne Lenhart[5], Johnny T. Ottesen[6,7]*

1 Institute of Mathematics, University of the Philippines Diliman, Quezon City, Philippines, **2** Maritime Academy of Asia and the Pacific, Bataan, Philippines, **3** Biomedical Mathematics Group, Pioneer Research Center for Mathematical and Computational Sciences, Institute for Basic Science, Daejeon, Republic of Korea, **4** Department of Mathematics, North Carolina State University, Raleigh, North Carolina, United States of America, **5** Department of Mathematics, University of Tennessee, Knoxville, Tennessee, United States of America, **6** Department of Sciences, Roskilde University, Roskilde, Denmark, **7** Center for Mathematical Modeling—Human Health and Diseases, Roskilde University, Roskilde, Denmark

* adlreyes@math.upd.edu.ph (AADLRV); johnny@ruc.dk (JTO)

Citation: Gavina BLA, de los Reyes V AA, Olufsen MS, Lenhart S, Ottesen JT (2023) Toward an optimal contraception dosing strategy. PLoS Comput Biol 19(4): e1010073. https://doi.org/10.1371/journal.pcbi.1010073

Editor: Krasimira Tsaneva-Atanasova, University of Exeter, UNITED KINGDOM

Received: April 3, 2022

Accepted: February 27, 2023

Published: April 13, 2023

Peer Review History: PLOS recognizes the benefits of transparency in the peer review process; therefore, we enable the publication of all of the content of peer review and author responses alongside final, published articles. The editorial history of this article is available here: https://doi.org/10.1371/journal.pcbi.1010073

Data Availability Statement: This manuscript uses data that are extracted from Fig 1 in Welt CK, McNicholl DJ, Taylor AE, Hall JE. Female reproductive aging is marked by decreased secretion of dimeric inhibin. J Clin Endocrinol

Abstract

Anovulation refers to a menstrual cycle characterized by the absence of ovulation. Exogenous hormones such as synthetic progesterone and estrogen have been used to attain this state to achieve contraception. However, large doses are associated with adverse effects such as increased risk for thrombosis and myocardial infarction. This study utilizes optimal control theory on a modified menstrual cycle model to determine the minimum total exogenous estrogen/progesterone dose, and timing of administration to induce anovulation. The mathematical model correctly predicts the mean daily levels of pituitary hormones *LH* and *FSH*, and ovarian hormones E_2, P_4, and *Inh* throughout a normal menstrual cycle and reflects the reduction in these hormone levels caused by exogenous estrogen and/or progesterone. Results show that it is possible to reduce the total dose by 92% in estrogen monotherapy, 43% in progesterone monotherapy, and that it is most effective to deliver the estrogen contraceptive in the mid follicular phase. Finally, we show that by combining estrogen and progesterone the dose can be lowered even more. These results may give clinicians insights into optimal formulations and schedule of therapy that can suppress ovulation.

Author summary

Hormonal contraceptives composed of exogenous estrogen and/or progesterone are commonly administered artificial means of birth control. Despite many benefits, adverse side effects associated with high doses such as thrombosis and myocardial infarction, cause hesitation to usage. Our study presents an improved mathematical model for hormonal control of the menstrual cycle and applies optimal control theory to minimize total exogenous estrogen and/or progesterone dose, and determine timing of administration that lead to contraception. We observe a reduction in dosage of about 92% in estrogen monotherapy and 43% in progesterone monotherapy. Our simulations show that it is most

Metab. 1999;84:105-111, using the software DigitizeIt version 2.5 by Bormann I available from https://www.digitizeit.xyz/. The extracted data has been included in the supplementary material. Optimization and parameter estimation codes are accessible through the link https://github.com/3r3nd/menstrual-cycle-project.

Funding: BLAG was supported by University of the Philippines Office of International Linkages, a Continuous Operational and Outcomes-based Partnership for Excellence in Research and Academic Training Enhancement (UP-OIL-COOPERATE) grant, and a Commission on Higher Education Faculty Development Program - II (CHED-FDP-II) scholarship. AADLRV acknowledges the support of the Institute of Mathematics, University of the Philippines Diliman and the Institute for Basic Science (IBS-R029-C3). The funders had no role in study design, data collection and analysis, decision to publish, or preparation of the manuscript.

Competing interests: The authors have declared that no competing interests exist.

effective to deliver the estrogen contraceptive in the mid follicular phase. In addition, we illustrate that combination therapy significantly lower doses further. Our findings may give clinicians insights into optimal dosing scheme for contraception.

Introduction

The female's reproductive life spanning approximately 39 years from age of 12.5 until 51 is governed by the menstrual cycle [1], a cyclic process regulated by the endocrine system. A normal menstrual cycle involves ovarian follicular development, ovulation, and luteinization influenced by the hormones gonadotropin-releasing hormone (GnRH), luteinizing hormone (*LH*), follicle-stimulating hormone (*FSH*), estradiol (E_2), progesterone (P_4), and inhibin (*Inh*), which are produced in the hypothalamus, pituitary, and ovaries [2, 3]. During this cycle, the pituitary and ovarian hormones fluctuate. Unusual concentrations of these hormones lead to abnormal cycles. For instance, low levels of *LH*, *FSH*, and E_2 cause anovulation [3]. Anovulation is an abnormal menstrual cycle characterized by the absence of the ovulation process [4].

Numerous previous modeling studies have examined the menstrual cycle, how it is formed and how it can be altered. The most significant body of work stems from Selgrade et al. [5–13]. These studies start by developing a continuous menstrual cycle model and fitting it to data. This model consists of two parts tracking the pituitary [6] and ovarian [5] portions of the cycle. The full model developed by Harris et al. [7, 8, 12] is formulated as an autonomous nonlinear system of 13 delay differential equations (DDEs) merging the pituitary and ovarian components. The model, consisting of positive and negative feedback relationships of the pituitary and ovarian hormones, was fitted to data from McLachlan et al. [14] reporting daily blood concentrations of *LH*, *FSH*, E_2, P_4, and *Inh* averaged from data for 33 normally cycling women. Pasteur [9] expanded this model distinguishing the effect of inhibin A (*Inh A*) and inhibin B (*Inh B*). The inclusion of the two forms of inhibin provides a more realistic representation of the human menstrual cycle since these hormones are active in different phases of the cycle [9]. The model was further developed in the study by Margolskee et al. [11] who reduced the number of delays to one (delay in inhibin) and fitted it to data by Welt et al. [15], which consist of daily mean blood levels of *LH*, *FSH*, E_2, P_4, and *Inh A* averaged over 23 normally cycling women. Most recently, Wright et al. [13] added autocrine mechanisms to the Margolskee model to describe the influence of exogenous estrogen and/or progesterone in perturbing a normal cycle to contraceptive state.

In addition to work by Selgrade and collaborators, Chen et al. [16] introduced a simple model with three delay differential equations describing the hormonal interactions of the human menstrual cycle along the hypothalamus-pituitary-ovaries axis. Reinecke et al. [17, 18] studied the pulsatile release of GnRH in the hypothalamus using a stochastic process, and Röblitz et al. [19] utilized ordinary differential equations (ODEs) to examine the interactions between GnRH, pituitary, and ovarian hormones which shortened computational time.

These menstrual cycle models and their modifications, all fitted to biological data consisting of blood levels of pituitary and ovarian hormones from normally cycling women, have been used to study fertility [7, 9, 12, 19], reproductive diseases [16], and contraception [13, 17–19]. For instance, Pasteur's model showed that the dosage of exogenous estrogen varies inversely as the amplitudes of hormone level fluctuations, while Chen's model simulated treatment of uterine myomas with GnRH analogues.

Contraception is achieved through natural and/or artificial means. Artificial methods include hormonal, barrier, permanent, and long-acting reversible contraceptives. Today,

contraception is most commonly achieved by taking a daily pill, though this method is rapidly being replaced by injectables and implants [20]. Independent of the administration method, almost all hormonal contraceptives including exogenous progesterone and/or estrogen act by blocking ovulation, changing cervical mucus, which hinders sperm transport and/or modifying endometrium which prevents implantation [21]. Aside from contraceptive benefit, suppression of ovulation can alleviate negative premenstrual symptoms [22–24] and reduce anterior cruciate ligament (ACL) injury [25, 26], among others. For example, Hammarbäck et al. [23] showed that cyclical negative premenstrual symptoms such as irritability and breast tenderness disappear in anovulatory cycles. In addition, Yonkers et al. [24] found that administration of GnRH analogues, exogenous estrogen, and certain oral contraceptives at doses which inhibit ovulation is effective in reducing the symptoms. The paper [27] reported that ACL injuries in female athletes are significantly greater during the ovulatory phase and studies [25, 28, 29] suggested that oral contraceptive users have an almost 20% decreased risk for ACL injury. Most literature studies [13, 18, 19] focus on the administration of exogenous hormones such as estrogen, progesterone, and GnRH analogues to inhibit ovulation. For example, Reinecke's detailed DDE model included a numerical study on the parts of body affected by estrogen and/or progesterone hormonal contraceptives. This model compared results from administering the contraceptive continuously at a constant rate and at certain time points. Röblitz's ODE model compares the effect of administering a single and multiple dose of Nafarelin (a GnRH agonist) and Cetrorelix (a GnRH antagonist known to impede ovulation in in-vitro fertilization treatment), and Wright's model simulated exogenous estrogen and/or progesterone doses concluding that by combining the two effectors the dose can be lowered significantly. These studies explored the effect of exogenous hormones for inducing anovulation but did not examine optimal dosing. With rapid advance in implants and injections providing continuous administration there is great potential to implement new patient-specific minimizing dosing schemes. To our knowledge, our work is the first to use modeling to study timing of dosing thereby minimizing the dose even more. As implants become more common, results from this study have the potential to provide contraception to more women, in particular since lower doses also decrease the risks for adverse side effects such as venous thromboembolism and myocardial infarction associated with high doses of hormonal contraceptives [3, 30–32].

While optimal control theory has not been used to simulate contraception, the theory has long tradition in biology to find strategies that optimize an outcome. In [33], the theory is applied to a system of ODEs to determine a scheme for delivery of insulin and glucagon that regulates blood glucose level in diabetes patients. The study [34] utilized optimal control to develop treatment protocol for tumor stabilization for prostate cancer. Several studies explore optimization of hormonal treatments. For instance, [35] described an optimal dosing regimen for the infusion of *FSH* to patients undergoing in vitro fertilization. While in [36], control theory is employed to investigate optimal dosage decisions in the administration of gonadotropin in controlled ovarian hyperstimulation treatment cycle. The current paper expands previously published papers by Selgrade et al. on the hormonal regulation of the menstrual cycle [7, 12] and the transition to contraception [13]. In this study, the model in Margolskee and Selgrade [11] is modified to include mechanisms depicting the contraceptive effect of exogenous progesterone on the menstrual cycle. This new model shows the principal mechanisms behind transition to contraception. It is calibrated to the patient-data extracted from Welt et al. [15] and predicts the daily levels of pituitary hormones *LH* and *FSH*, and ovarian hormones E_2, P_4, and *Inh* averaged during a normal menstrual cycle in 23 women. The model output also predicts reduction in pituitary and ovarian hormone levels caused by exogenous estrogen and/or progesterone observed by Obruca et al. [37] and Deb et al. [38].

This paper uses an optimal control approach to simulate contraception using the model described above. The objective is to identify strategies to understand when and how much estrogen and/or progesterone to administer to obtain a contraceptive state. Results show that the dosage may be reduced by 92% in estrogen monotherapy, 43% in progesterone monotherapy, to suppress ovulation. Simulations agree with biological literature that in monotherapy, administration of estrogen in the mid follicular phase is effective at preventing ovulation. Lastly, numerical experiments show that by combining estrogen and progesterone the dose can be reduced even further. The results of this study may aid in identifying the minimum dose and treatment schedule that cause anovulation.

Materials and methods

This section describes the normal and anovulatory menstrual cycle, data, the mathematical model, parameter estimation, and optimal control method. Table 1 lists the state variables in the mathematical model. The model parameters and their values are given in Table B in S1 Text.

The normal menstrual cycle

The normal menstrual cycle (shown in Fig 1) for an adult female has an average length of 28 days. It has two stages, the follicular phase and luteal phase. Through hormones, the hypothalamus, pituitary, and ovaries interact to regulate the menstrual cycle [2, 3].

During the menstrual cycle, the hypothalamus produces pulses of GnRH which control pituitary's secretion of the gonadotropins *FSH* and *LH*. At the beginning of the follicular phase (the start of menstruation or menses), *FSH* rises and causes the recruitment of a group of immature follicles. As these follicles develop through the stimulation of the gonadotropins *FSH* and *LH*, they increase secretion of E_2 (see Fig 2). Follicular development is indicated by an enlargement of oocyte (immature egg), multiplication, and transformation of granulosa cells (structure that surrounds the oocyte) to a cuboidal shape, and formation of small gap junctions, which enable nutritional, metabolite, and signal interchange between the granulosa cells and oocyte [3]. Toward the end of the follicular stage, one dominant follicle continues to grow while the rest of the follicles become atretic. As the dominant follicle grows, the E_2 level

Table 1. Menstrual cycle state variables and initial conditions.

State variable	Description	Initial condition	Unit	Reference
RP_{LH}	Amount of reserve pool *LH*	167.57	IU	estimated
LH	*LH* blood concentration	11.81	IU/L	estimated
RP_{FSH}	Amount of reserve pool *FSH*	14.48	IU	estimated
FSH	*FSH* blood concentration	11.41	IU/L	estimated
RcF	Amount of active follicular mass in the recruited follicular stage	2.10	ng	estimated
GrF	in the growing follicular stage	4.12	ng	estimated
$DomF$	in the dominant follicular stage	0.46	ng	estimated
Sc_1	during ovulation	1.06	ng	estimated
Sc_2	during luteinization	1.67	ng	estimated
Lut_1	Amount of active luteal mass in the first luteal stage	4.16	ng	estimated
Lut_2	in the second luteal stage	13.03	ng	estimated
Lut_3	in the third luteal stage	16.48	ng	estimated
Lut_4	in the fourth luteal stage	10.29	ng	estimated

https://doi.org/10.1371/journal.pcbi.1010073.t001

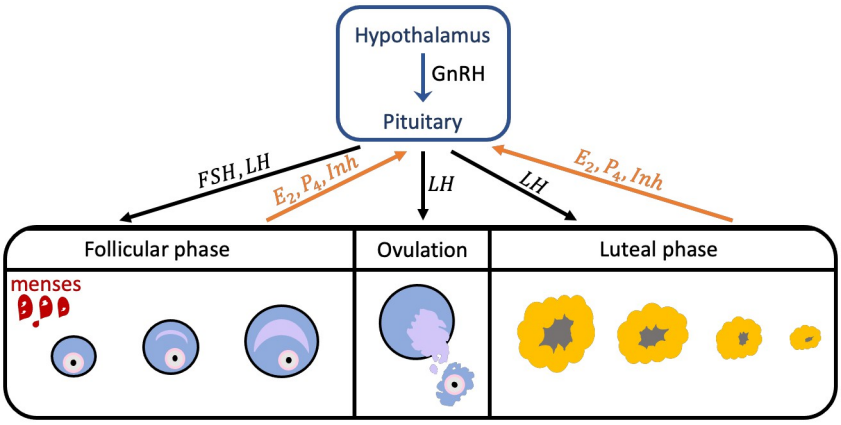

Fig 1. The Follicular and Luteal Phases of the menstrual cycle. The figure shows the transition of a follicle, from its growth in the follicular phase to its rupture during ovulation, as well as its transformation to a corpus luteum and degradation in the luteal phase. The blue arrow indicates the control of the hypothalamus in the secretion of pituitary hormones. The black arrows represent the influence of the pituitary system on the ovarian system through *FSH* and *LH*, and the orange arrows show the response of the ovarian system through E_2, P_4, and *Inh*.

https://doi.org/10.1371/journal.pcbi.1010073.g001

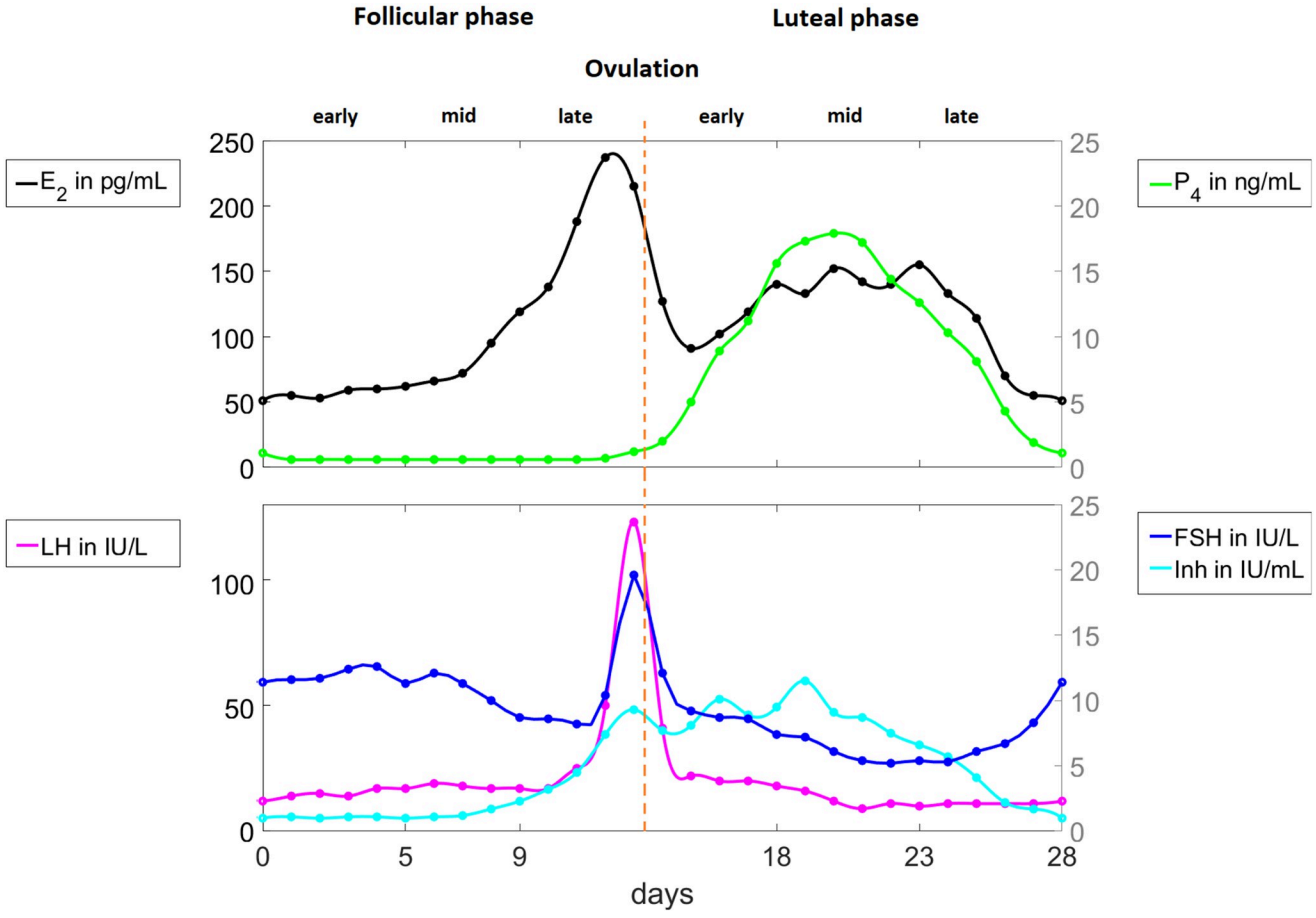

Fig 2. Pituitary and ovarian hormone levels in a normal menstrual cycle. Data digitized from the study by Welt et al. [15] is interpolated by cubic splines. The hormones *LH*, *FSH*, and E_2 peak in the late follicular phase while P_4 and *Inh* reach maximum value in the luteal phase.

https://doi.org/10.1371/journal.pcbi.1010073.g002

increases to a maximum value prompting an *LH* surge. The *LH* surge stimulates ovulation, releasing the egg from the dominant follicle. The ruptured dominant follicle then transforms to a corpus luteum. As the corpus luteum grows, P_4 and *Inh* production is increased. P_4 and *Inh* inhibit the synthesis of *LH* and *FSH*. If fertilization does not occur, the corpus luteum degrades removing the inhibition on *LH* and *FSH*. Consequently, levels of *FSH* and *LH* rise and the menstrual cycle repeats [2, 3].

The anovulatory cycle and contraception

Anovulation occurs when the follicle fails to release the egg. This state can be detected by measuring serum progesterone. During a normal menstrual cycle, progesterone is largely produced by the corpus luteum after ovulation. Its levels stay below 2 ng/mL during the follicular phase and peak 7 to 8 days after ovulation [3]. Accordingly, a low concentration of this hormone in the luteal phase indicates anovulation or defective luteinization [39]. The menstrual cycle is classified as anovulatory if progesterone concentration remains below 5 ng/mL without an *LH* peak [40]. In fact, disruption at any level of the hypothalamic-pituitary-gonadal axis can result in anovulation. This includes suppression of GnRH, the presence of a pituitary tumor leading to gonadotropin secretory dynamics that fail to stimulate follicular growth, or abnormal estrogen feedback signaling causing inhibition of *FSH* secretion or a low estrogen level which prevent the *LH* surge [3].

Hormonal contraceptives, composed of progesterone alone, or a combination of estrogen and progesterone are widely used artificial means of contraception. They are delivered orally, transdermally, vaginally, via implants, or injections. Estrogen or progesterone alone can cause contraception via anovulation but the combined administration of both hormones significantly enhances effectiveness [41].

In oral steroid contraceptives composed of both exogenous estrogen and progesterone, progesterone induces anovulation by preventing the midcycle rise in *LH* secretion [41, 42]. This is due to progesterone's suppression of follicular development and gonadotropin secretion [43]. The insufficient *FSH* prevents follicle growth. Consequently, the lack of follicle growth results in an inadequate amount of estradiol inhibiting the *LH* surge [3]. The estrogen component suppresses *FSH* secretion blocking folliculogenesis, stabilizing the endometrium, which minimize bleeding [42, 44].

Data

The output of the mathematical model without the administration of exogenous hormone is compared to the 28-day data (solid circles in Fig 2) from Welt et al. [15]. These data (see Table A in S1 Text), extracted from Fig 1 in [15] using the software DigitizeIt version 2.5 [45], comprise mean levels of E_2, P_4, *Inh A*, *LH*, and *FSH* taken from 23 normally cycling younger women aged 20 to 34 years, all with a history of a regular 25–35 day menstrual cycle with evidence of ovulation in the preceding cycle. Our study employs only *Inh A* since *Inh B* is more significant in studies about reproductive aging. The Welt study [15] reports that the data are centered to the day of ovulation requiring three of the following four criteria to be satisfied: i) LH peak day, ii) midcycle FSH peak day, iii) the day of or after the midcycle E_2 peak, and iv) day that the P_4 doubled from its baseline or reached a level of 0.6 ng/mL. Before averaging the data the menstrual cycle data were standardized to a 28-day cycle length with the day of ovulation centered to day 0 and the mean hormone levels were averaged over the early, mid-, and late follicular phase and early, mid-, and late luteal phase, see [15] for more details.

Mathematical model of the normal menstrual cycle

To study anovulation, we use the normal menstrual cycle model by Margolskee et al. [11] and induce anovulation via added estrogen and progesterone. The core model, shown in Fig 3, includes the pituitary and ovarian phases. It assumes that

a.1 *LH* and *FSH* synthesis occurs in the pituitary,

a.2 *LH* and *FSH* are held in a reserve pool awaiting release into the bloodstream, and

a.3 the follicular/luteal mass undergoes nine ovarian stages of development.

In the model, $RP_{LH}(t)$ and $RP_{FSH}(t)$ denote the amount of *LH* and *FSH* in the reserve pool at time *t* days, $LH(t)$ and $FSH(t)$ are the blood concentrations of *LH* and *FSH*; $E_2(t)$, $P_4(t)$, and $Inh(t)$ denote the blood levels of E_2, P_4, and *Inh*; and $RcF(t)$, $GrF(t)$, $DomF(t)$, $Sc_1(t)$, $Sc_2(t)$, $Lut_1(t)$, $Lut_2(t)$, $Lut_3(t)$, and $Lut_4(t)$ are the masses of active follicular/luteal tissues in the nine ovarian stages: recruited, growing, and dominant follicular stages, ovulation, luteinization, first, second, third, and fourth stages of luteal development.

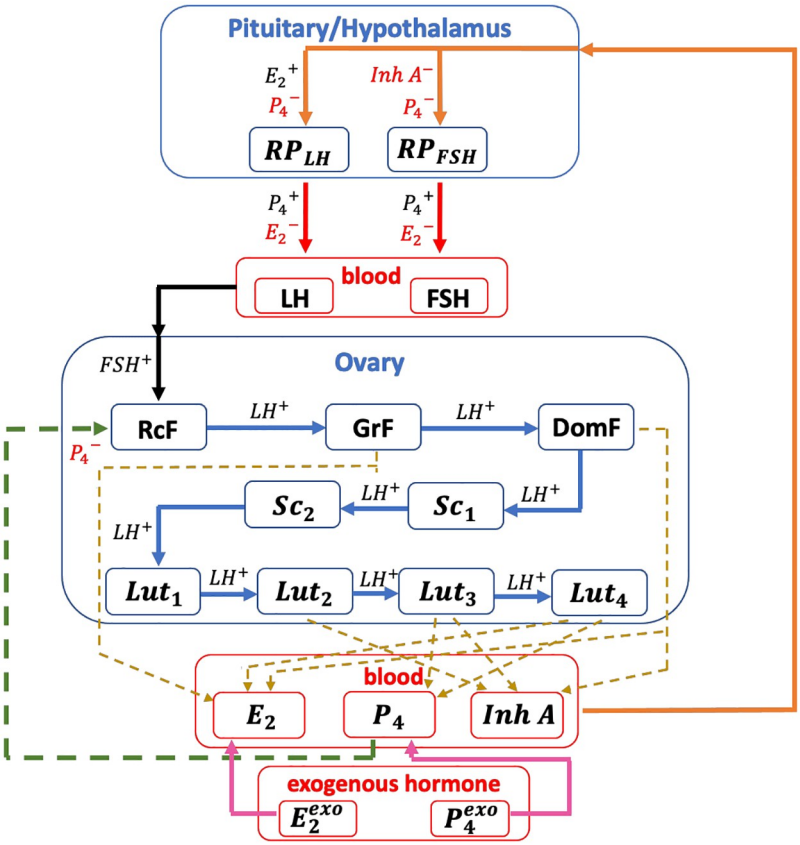

Fig 3. Model diagram. The diagram (adapted from [13]) shows the 13 states (RP_{LH}, RP_{FSH}, *LH*, *FSH*, *RcF*, *GrF*, *DomF*, Sc_1, Sc_2, Lut_1, Lut_2, Lut_3, Lut_4) in the menstrual cycle model. H^+ denotes stimulation by hormone *H* while H^- denotes inhibition. The red arrow presents the release of the pituitary hormone from the reserve pool to the blood. The black arrow indicates the influence of the pituitary system on the ovarian system while the orange arrow denotes the ovary's feedback. The green dashed arrow denotes inhibition of P_4 in the *RcF* stage. The blue arrow describes the transition of a follicle from one ovarian stage to the next. The gold dashed arrow denotes the state contributing to the ovarian hormone production. The pink arrow represents the infusion of exogenous hormone to the ovarian system.

https://doi.org/10.1371/journal.pcbi.1010073.g003

The pituitary model includes the hypothalamus and the pituitary. It predicts the synthesis, release, and clearance of *LH* and *FSH*, and the pituitary's response to E_2, P_4, and *Inh* (see Fig 3). The direct effect of the ovarian hormones on the pituitary and indirect influence via the hypothalamus are grouped partly because of the complexity of tracking GnRH [6].

The rate of change of $RP_{LH}(t)$ in Eq (1) is the difference between two terms. The first term describes the synthesis in the pituitary and the second term represents the release of *LH* into the blood. A Hill function is used in the synthesis term of *LH* to predict the strong stimulatory effect for E_2 levels above the threshold level Km_{LH}. P_4 inhibits the production but bolsters the *LH* release into the bloodstream. E_2 inhibits the release of *LH*. The change in $LH(t)$ in Eq (2) is affected by the *LH* release into and clearance from the blood. The *LH* release rate is assumed proportional to its amount in the reserve pool, while the clearance rate is proportional to the *LH* blood level.

Likewise, the rate of change of $RP_{FSH}(t)$ in Eq (3) is governed by synthesis and release. The synthesis of *FSH* is inhibited by both *Inh* and P_4. The time delay τ is introduced to account for the time it takes the *FSH* synthesis rate to respond to changes in the *Inh* concentration. P_4 stimulates the *FSH* release into the bloodstream. The quadratic expression E_2^2 in the *FSH* release term is included to ensure greater inhibitory effect of E_2 on *FSH* release than on *LH* release. Similarly, the rate of change of $FSH(t)$ in Eq (4) depends on two terms: a release term assumed proportional to the amount of *FSH* in the reserve pool and a clearance term assumed proportional to the *FSH* blood concentration.

Applying this model to the hormone cascade described above, gives the following system of DDEs

$$\frac{d}{dt}RP_{LH}(t) = \frac{V_{0,LH} + \frac{V_{1,LH}E_2(t)^8}{Km_{LH}^8 + E_2(t)^8}}{1 + P_4(t)/Ki_{LH,P}} - \frac{k_{LH}[1 + c_{LH,P}P_4(t)]RP_{LH}(t)}{1 + c_{LH,E}E_2(t)}, \tag{1}$$

$$\frac{d}{dt}LH(t) = \frac{1}{v}\frac{k_{LH}[1 + c_{LH,P}P_4(t)]RP_{LH}(t)}{1 + c_{LH,E}E_2(t)} - \alpha_{LH}LH(t), \tag{2}$$

$$\frac{d}{dt}RP_{FSH}(t) = \frac{V_{FSH}}{1 + Inh(t-\tau)/Ki_{FSH,Inh} + P_4(t)/w} - \frac{k_{FSH}[1 + c_{FSH,P}P_4(t)]RP_{FSH}(t)}{1 + c_{FSH,E}E_2(t)^2}, \tag{3}$$

$$\frac{d}{dt}FSH(t) = \frac{1}{v}\frac{k_{FSH}[1 + c_{FSH,P}P_4(t)]RP_{FSH}(t)}{1 + c_{FSH,E}E_2(t)^2} - \alpha_{FSH}FSH(t). \tag{4}$$

The ovarian model predicts the response of the ovarian hormones E_2, P_4, and *Inh* as functions of *LH* and *FSH*.

The rate of change of the mass of active follicular/luteal tissue in Eqs (5) to (13) depends on the mass of follicular/luteal tissue promoted to that stage and the mass advancing to the next stage. *FSH* in Eq (5) stimulates, while P_4 inhibits, the recruitment of immature follicles to the *RcF* stage. *LH* in Eqs (5) to (7) aids the growth and transition of follicles to the next follicular stage until ovulation.

The rate of production of hormones at each ovarian stage is assumed proportional to the active mass of the follicle or corpus luteum at that stage. Furthermore, the blood concentrations of the ovarian hormones are assumed at a quasi-steady state because the clearance of ovarian hormones from the blood is faster than the clearance of pituitary hormones and the time scale for follicular and luteal development. Thus, the blood concentration of each ovarian hormone in Eqs (14) to (16) is written as linear combinations of follicular/luteal masses in the

stages secreting it [5, 11, 12, 17]. The constants b_1 and b_2 in Eqs (14) and (15) reflect the functions of exogenous estrogen $E_2^{exo}(t)$ and progesterone $P_4^{exo}(t)$, given as blood concentrations, which may be different from endogenous hormones. The exact influence of the exogenous hormones on the endogenous hormone levels are not incorporated and thus we let $b_1 = 1$ and $b_2 = 1$ agreeing with the mathematical model published in [7, 12, 13]. Eqs (5) to (16) reflect the transition of follicular/luteal mass from recruitment, to ovulation, to the stages of the luteal phase, and the effect of the pituitary to the ovarian hormones, given by the following ordinary differential equations

$$\frac{d}{dt}RcF(t) = (b + c_1 RcF(t))\frac{FSH(t)}{1 + P_4(t)/q} - c_2 LH(t)^{\alpha} RcF(t), \tag{5}$$

$$\frac{d}{dt}GrF(t) = c_2 LH(t)^{\alpha} RcF(t) - c_3 LH(t) GrF(t), \tag{6}$$

$$\frac{d}{dt}DomF(t) = c_3 LH(t) GrF(t) - c_4 LH(t)^{\gamma} DomF(t), \tag{7}$$

$$\frac{d}{dt}Sc_1(t) = c_4 LH(t)^{\gamma} DomF(t) - d_1 Sc_1(t), \tag{8}$$

$$\frac{d}{dt}Sc_2(t) = d_1 Sc_1(t) - d_2 Sc_2(t), \tag{9}$$

$$\frac{d}{dt}Lut_1(t) = d_2 Sc_2(t) - k_1 Lut_1(t), \tag{10}$$

$$\frac{d}{dt}Lut_2(t) = k_1 Lut_1(t) - k_2 Lut_2(t), \tag{11}$$

$$\frac{d}{dt}Lut_3(t) = k_2 Lut_2(t) - k_3 Lut_3(t), \tag{12}$$

$$\frac{d}{dt}Lut_4(t) = k_3 Lut_3(t) - k_4 Lut_4(t), \tag{13}$$

with auxiliary equations

$$E_2(t) = e_0 + e_1 GrF(t) + e_2 DomF(t) + e_3 Lut_4(t) + b_1 E_2^{exo}(t), \tag{14}$$

$$P_4(t) = p_0 + p_1 Lut_3(t) + p_2 Lut_4(t) + b_2 P_4^{exo}(t), \tag{15}$$

and

$$Inh(t) = h_0 + h_1 DomF(t) + h_2 Lut_2(t) + h_3 Lut_3(t). \tag{16}$$

Novel model modifications: Anovulatory cycle and contraception

Exogenous estrogen and/or progesterone inhibit ovulation through different mechanisms. Estrogen causes anovulation by suppressing gonadotropin secretion, depicted in the release term of Eqs (1) and (3). Low gonadotropin levels inhibit maturation of follicles causing low

production of estrogen insufficient to induce an *LH* surge. The administration of progesterone reduces ovarian hormone levels [37]. The Margolskee model [11] is unable to reflect this condition. Therefore, to attain contraceptive effect of progesterone we included the following terms accounting for

b.1 $\frac{P_4(t)}{w}$ in the synthesis term of Eq (3) and

b.2 $\frac{P_4(t)}{q}$ in the first term of Eq (5).

The term $\frac{P_4(t)}{q}$ describes the direct inhibitory action of progesterone on follicular development [43, 46]. Baird et al. [43] and Setty et al. [46] also suggested that reduced follicle growth is further caused by the suppression of gonadotropin secretion. Moreover, Batra et al. [47] found that in ovine pituitary cell culture, progesterone decreases *FSH* secretion through decreased *FSH* biosynthesis. This inhibition of *FSH* production is accounted for by the term $\frac{P_4(t)}{w}$. In the model, the administration of both $E_2^{\text{exo}}(t)$ and $P_4^{\text{exo}}(t)$ increases suppression of gonadotropin secretion. This leads to lower combined doses to induce anovulation, showing the enhanced effectivity of combined treatment suggested in Rivera et al. [41].

Parameter estimation

To calibrate the model to the data extracted from Welt et al. [15], we estimated selected model parameters as follows:

c.1 The parameters in the pituitary model (Eqs (1), (2) and (3) (without $P_4(t)/w$), and (4)) are estimated starting from parameter values and initial conditions in [11]. For this submodel, we replaced $E_2(t)$, $P_4(t)$, and $Inh(t)$ by time-dependent functions fitted to E_2, P_4, and *Inh* levels in the data extracted from Welt et al. [15].

c.2 The parameters in the ovarian model (Eqs (5) (without $P_4(t)/q$) to (13), (14) (with $E_2^{\text{exo}}(t) = 0$), (15) (with $P_4^{\text{exo}}(t) = 0$), and (16)) are estimated starting with parameter values and initial conditions in [11]. For this submodel, we substituted $LH(t)$ and $FSH(t)$ by time-dependent functions fitted to *LH* and *FSH* levels in data extracted from Welt et al. [15].

c.3 The parameters obtained in c.1 and c.2 are used to estimate the parameters in the merged pituitary and ovarian model.

c.4 We do not have physiological knowledge of the parameters w and q thus, values assigned to w and q with order of magnitude between 0 and 1, and the parameter set obtained in c.3 are used as initial guess to estimate parameters in the final merged model.

In **c.1** to **c.4** we used the MATLAB `fminsearch` function, which utilizes the Nelder-Mead simplex algorithm, to estimate parameters that minimize least squares error. The least squares function employed in c.4 is

$$\frac{1}{M-N}\sum_{i=1}^{M}\left(w_{E_2^*}(i)\left((E_2(i)-E_2^*(i))\frac{1}{E_2^*(i)}\right)^2+w_{P_4^*}(i)\left((P_4(i)-P_4^*(i))\frac{1}{P_4^*(i)}\right)^2\right.$$
$$+w_{Inh^*}(i)\left((Inh(i)-Inh^*(i))\frac{1}{Inh^*(i)}\right)^2+w_{LH^*}(i)\left((LH(i)-LH^*(i))\frac{1}{LH^*(i)}\right)^2$$
$$\left.+w_{FSH^*}(i)\left((FSH(i)-FSH^*(i))\frac{1}{FSH^*(i)}\right)^2\right),$$

where $H(i)$ is the hormone model output at day i, and $H^*(i)$ is the hormone Welt data at day i for hormones E_2, P_4, *Inh*, *LH*, and *FSH*. The weight $w_{H^*}(i)$ equals 1 except for:

i. $w_{E_2^*}(13) = 1.58$, the z-score of 13th E_2 data (the maximum E_2 data),

ii. $w_{P_4^*}(21) = 1.39$, the z-score of 21th P_4 data (the maximum P_4 data),

iii. $w_{Inh^*}(20) = 1.35$, the z-score of 20th *Inh* data (the maximum *Inh* data),

iv. $w_{LH^*}(14) = 2.16$, the z-score of 14th *LH* data (the maximum *LH* data), and

v. $w_{FSH^*}(14) = 1.80$, the z-score of 14th *FSH* data (the maximum *FSH* data).

M is the number of data points and N is the combined number of model parameters and initial conditions. The Welt data was standardized to 28 days. We used four repetitions of this data as shown in Fig 4 to obtain M data points utilized in parameter estimation. This is done to obtain a periodic solution. The difference $M - N$ in the denominator ascertains that errors don't increase with repetition of the data set. Because the hormones have different units, the multiplier $\frac{1}{H^*(i)}$ is used to obtain the term $(H(i) - H^*(i))\frac{1}{H^*(i)}$, the percentage error for hormone H. This eliminates the order of magnitude difference between the variables, allowing addition of residuals in the objective function. The *z–score*, denoting the number of standard deviations a data point is from the mean, aids in approximating the maximum hormone data. Manual adjustments after optimization are carried out to reach the maximum E_2, P_4, *Inh*, *LH*, and *FSH*, and to obtain cycle length close to the data cycle length of 28 days. This is essential since an anovulatory cycle is determined by the decrease in P_4 and *LH* maximum levels from the values in a normal cycle. The resulting initial conditions and parameter values are shown in Table 1 and Table B in S1 Text.

Optimal control applied to the menstrual cycle model

Optimal control theory describes control strategies to steer a system towards an optimal outcome specified in a cost function [48, 49]. In an optimal control problem, state variables $x(t)$ depending on time t, model a dynamical system and appropriate control function $u(t)$ is obtained by optimizing an objective function $J(u)$ subject to constraints [49]. In particular, consider the optimal control problem which minimizes an objective function $J(u)$ to determine optimal $u(t)$ and corresponding $x(t)$. Mathematically, it can be written as

$$\min_{u(t)} J(u) = \min_{u(t)} \int_{t_0}^{t_f} f(t, x(t), u(t))\, dt$$

subject to $x'(t) = g(t, x(t), u(t))$ and $x(t_0) = x_0$.

In this study, we let $u_1(t) = E_2^{\text{exo}}(t)$, $u_2(t) = P_4^{\text{exo}}(t)$, and

$$x(t) = (RP_{LH}(t), LH(t), RP_{FSH}(t), FSH(t), RcF(t), GrF(t), DomF(t), Sc_1(t), Sc_2(t), Lut_1(t), Lut_2(t), Lut_3(t), Lut_4(t)).$$

The objective is to seek minimum dosage for $u_1(t)$ and $u_2(t)$ which decreases the P_4 peak to a value resulting in an anovulatory state. That is,

$$\min_{u_1(t),u_2(t)} J(u) = \min_{u_1(t),u_2(t)} \int_{t_0}^{t_f} ((P_4(t) - P_0)^2 + a_1 u_1 + a_2 u_2^4) dt$$

subject to the model $x'(t) = g(t, t - \tau, x(t), u_1(t), u_2(t))$ and $x(t_0) = x_0$.

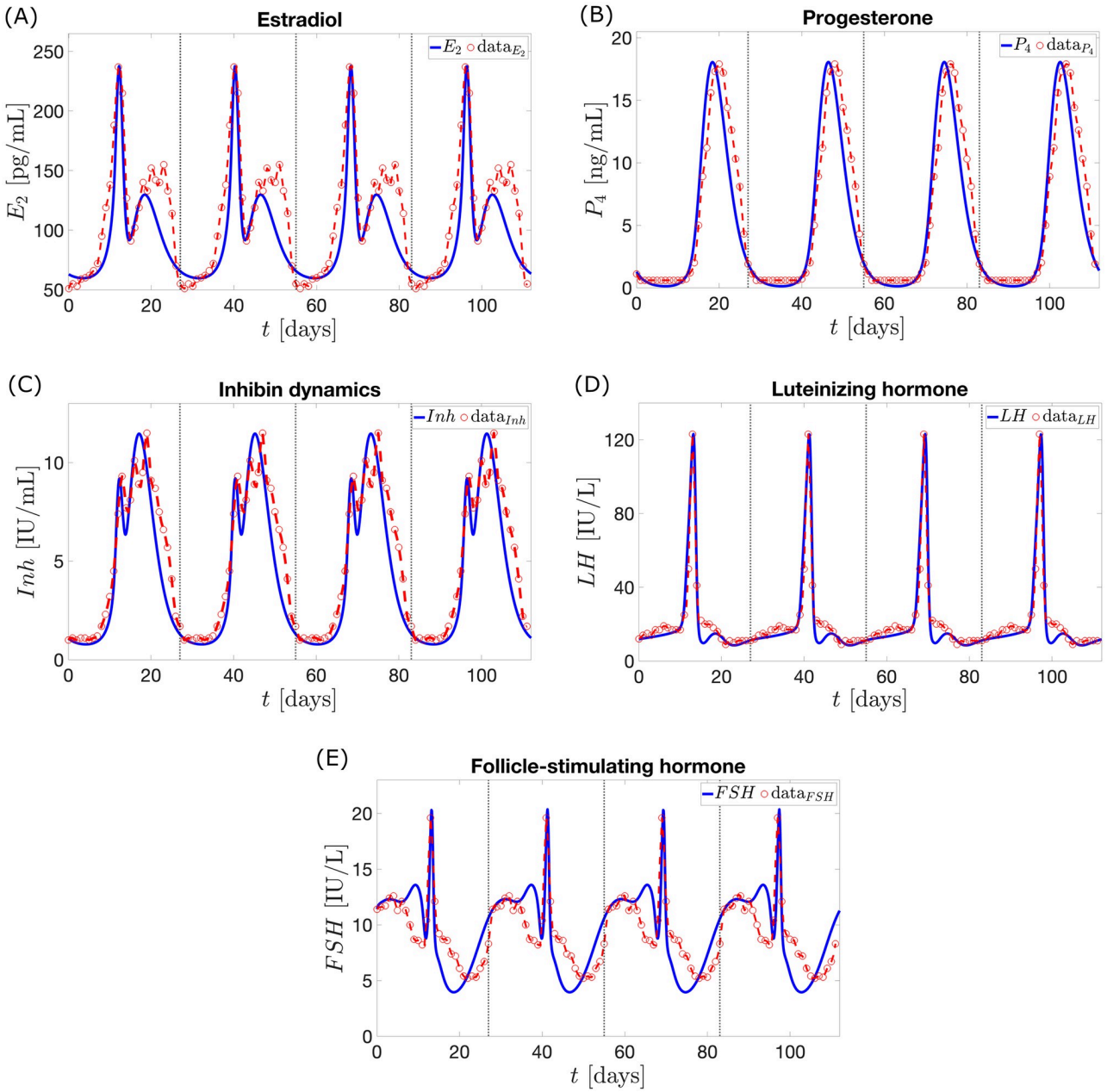

Fig 4. Normal cycle solution. The blue curves describe the dynamics of the pituitary and ovarian hormones predicted by the model without exogenous estrogen and progesterone. The vertical lines partition the red curves into four cycles. Each partition presents the 28-day normal cycle hormone data extracted from Welt et al. [15].

https://doi.org/10.1371/journal.pcbi.1010073.g004

The term $(P_4(t) - P_0)^2$ in the integrand is standard for getting $P_4(t)$ to track the target P_0 [50]. Because we want to keep $P_4(t) < 5$ ng/mL for $0 = t_0 < t_f = 28$, a target point P_0 must be lower than 5 ng/mL. In addition, simulations for constant dosage show that lowering P_4 level further requires higher dose of exogenous hormones. Thus, we take $P_0 = 4$ ng/mL, a value lower than but close to 5 ng/mL as target point. The second and third terms are included to minimize the dosage of exogenous hormones. The power of u_2 is 4 in order to add convexity to the optimal control problem and to smoothen the control. We have made an exhaustive investigation

of the powers of u_1 and u_2 in the objective function which presented results with least oscillation (few examples are shown in Fig C to Fig H in S1 Text). To identify the best objective function, we started with linear u_1 and u_2 cost terms. However, this form produced oscillatory results. Several runs revealed that the oscillations where the highest for optimal progesterone results. Thus, we increased the exponent of u_2 in the cost function and settled for a fourth power to smoothen the optimization results. To further smoothen results other methods may be explored like varying initial conditions and number of time points. The constants $a_1 > 0$ and $a_2 > 0$ are weight factors which balance the effort of minimizing u_1 and u_2, and hitting P_0. Random values with order of magnitude between −2 and 1 are originally assigned as initial guesses for the weights. If these weights produced P_4 peak higher than 5 ng/mL, their values are adjusted down. This iterative procedure was repeated until weights that make maximum $P_4(t) < 5$ ng/mL are obtained. We found that low values of weights produce small value of $\int_{t_0}^{t_f} (P_4(t) - P_0)^2 dt$ (see Table D in S1 Text), i.e., $P_4(t)$ is near P_0, but increases exogenous hormone dose.

To solve the optimal control problem we applied control parameterization. In this numerical method the control function is approximated by a linear combination of basis functions [48, 51]. Specifically, we utilize the MATLAB `makima` function which performs a piecewise cubic Hermite interpolation to estimate the control function. Moreover, we use `dde23` to solve the delay differential equations and `fmincon` to generate components of the piecewise cubic polynomial which gives the local least cost.

Exploring effects of exogenous hormones

To investigate the effect of exogenous estrogen and progesterone on the menstrual cycle, we compared

d.1 model output without exogenous hormone to data extracted from Welt et al. [15] for normally cycling women repeated four times,

d.2 model output with constant dose of exogenous hormone to hormone output in d.1, and

d.3 model output with optimal time-varying dose of exogenous hormone to hormone outputs in d.1 and d.2.

Some types of hormonal contraceptives like implants, injections, and patches are administered non-orally and continuously [21] while birth control pills are taken orally at specific time points. In **d.2** and **d.3** we study model response to exogenous estrogen and progesterone monotherapy, and combined treatment administered continuously for one cycle (28 days).

This study suggests a method/tool on how ovulation can be suppressed for an example woman with a specific cycle length. Though we are not presenting a population study, the method we described can be repeated to any woman if her hormone levels are known. To illustrate the adaptability of our method to women with different cycle lengths and understand how predictions change with variation in the period, we performed

e.1 sensitivity analysis (shown in Fig A in S1 Text) to determine the parameters which greatly affect the model cycle length, then

e.2 from the most sensitive parameters, we took some and vary them to make various cycle lengths, and

e.3 applied the optimization code to determine timing of administration and dosage of exogenous hormones that result in anovulation.

Table 2. Sum of squared residuals between the model output and Welt data, and model output peaks.

Hormone	Sum of squared residuals	Hormone peak		
		Hormone	Welt data	Model output
E_2	21840 (in pg^2/mL^2)	E_2 (in pg/mL)	237	238
P_4	183 (in ng^2/mL^2)	P_4 (in ng/mL)	17.9	18.1
Inh	66.6 (in IU^2/mL^2)	*Inh* (in IU/mL)	11.5	11.5
LH	1579 (in IU^2/L^2)	*LH* (in IU/L)	123	123
FSH	174 (in IU^2/L^2)	*FSH* (in IU/L)	19.6	20.4

https://doi.org/10.1371/journal.pcbi.1010073.t002

Results

This section presents the model output with and without administration of exogenous hormones. Sum of squared residuals between the model output without administration of exogenous hormones and Welt data, model output peak, and period are shown. In the administration of exogenous hormones, constant and time-varying doses are considered. Exogenous estrogen and progesterone monotherapies, and combination treatment of the two hormones are explored. For each type of therapy, minimum dose of exogenous estrogen and/or progesterone which leads to anovulation is determined. Optimal control theory is applied to investigate optimal time-varying doses.

The normal cycle solution

Without the administration of exogenous hormones ($E_2^{\text{exo}}(t) = 0$ and $P_4^{\text{exo}}(t) = 0$), the estimated initial condition in Table 1 produces a unique stable periodic solution (called the normal cycle solution) to the menstrual cycle model. The cycle length is 28.05 days (also see Table 2). Local stability of the solution is affirmed by varying the initial conditions.

Fig 4 depicts the dynamics of the ovarian and pituitary hormones E_2, P_4, *Inh*, *LH*, and *FSH* predicted by the model. It presents four cycles showing periodicity of the model output. The normal cycle solution (blue curve) exhibits hormone surges and dips and is a good estimate to the data extracted from Welt et al. [15] (red curve). Table 2 presents the sum of squared residuals between the model output and Welt data, and hormone output peaks.

Administration of exogenous hormones

Constant dosage. Exogenous estrogen and/or progesterone inhibits pituitary and ovarian maximum hormone levels [37, 38]. To simulate the response to a constant dose of exogenous estrogen monotherapy, $E_2^{\text{exo}}(t) = 20$ pg/mL per day and $P_4^{\text{exo}}(t) = 0$ are used in Eqs (14) and (15) for 28 days. Similarly, the effect of a constant dose of exogenous progesterone monotherapy is obtained with $P_4^{\text{exo}}(t) = 1.4$ ng/mL per day and $E_2^{\text{exo}}(t) = 0$. Table 3 presents the percentage

Table 3. Percentage decrease in model output peak with the administration of exogenous estrogen/progesterone.

Hormone	$E_2^{\text{exo}}(t) = 20$ pg/mL per day		$P_4^{\text{exo}}(t) = 1.4$ ng/mL per day	
	Current model	Wright model	Current model	Wright model
E_2 (in pg/mL)	21	16	51	81
P_4 (in ng/mL)	35	23	53	81
Inh (in IU/mL)	33	22	55	82
LH (in IU/L)	12	26	81	89
FSH (in IU/L)	9	13	35	29

https://doi.org/10.1371/journal.pcbi.1010073.t003

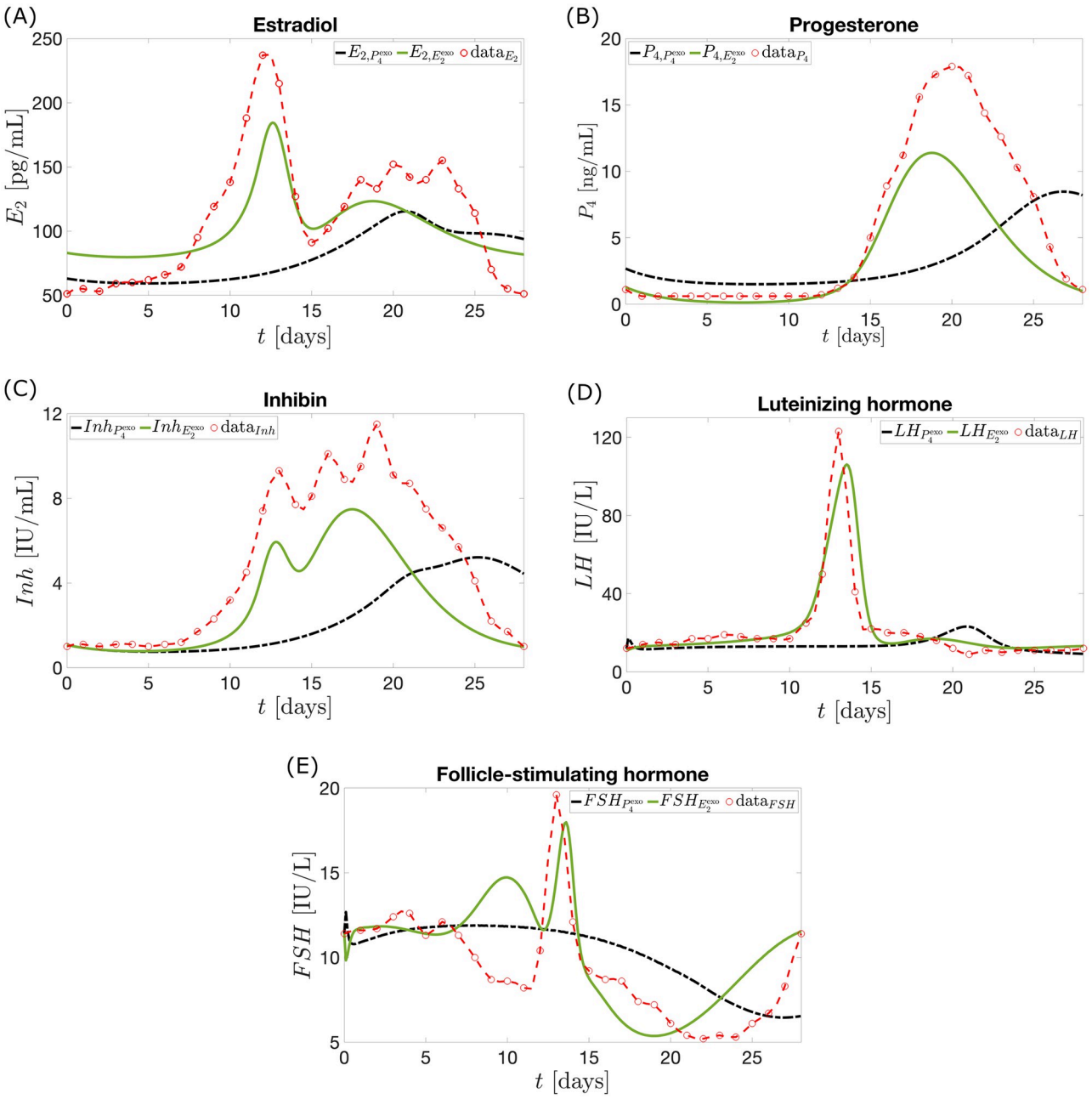

Fig 5. Model output with constant dose of exogenous hormone. $H_{P_4^{exo}}$ (black curve) or $H_{E_2^{exo}}$ (full green curve) is the hormone H model output in case of 20 pg/mL per day of exogenous E_2 or 1.4 ng/mL per day of exogenous P_4 is administered for 28 days, respectively. The stipulated red curve represents the data for the 28-day normal cycle extracted from Welt et al. [15]. The addition of exogenous E_2 or P_4 reduces the peak of each of the five hormones.

https://doi.org/10.1371/journal.pcbi.1010073.g005

decrease in model output peak compared to the hormone output peak of the Wright model of hormonal contraception [13]. The use of 20 pg/mL per day of estrogen or 1.4 ng/mL per day of progesterone results to the hormone profiles in Fig 5. Each of these amounts is insufficient to manifest anovulation because although reduced, the maximum P_4 value is still more than 5 ng/ml. To determine $E_2^{exo}(t)$ and $P_4^{exo}(t)$ values which block ovulation, we observe the LH and P_4 model output as the dosages vary from 0 to 60 pg/mL per day on a 0.1 pg/mL-interval for

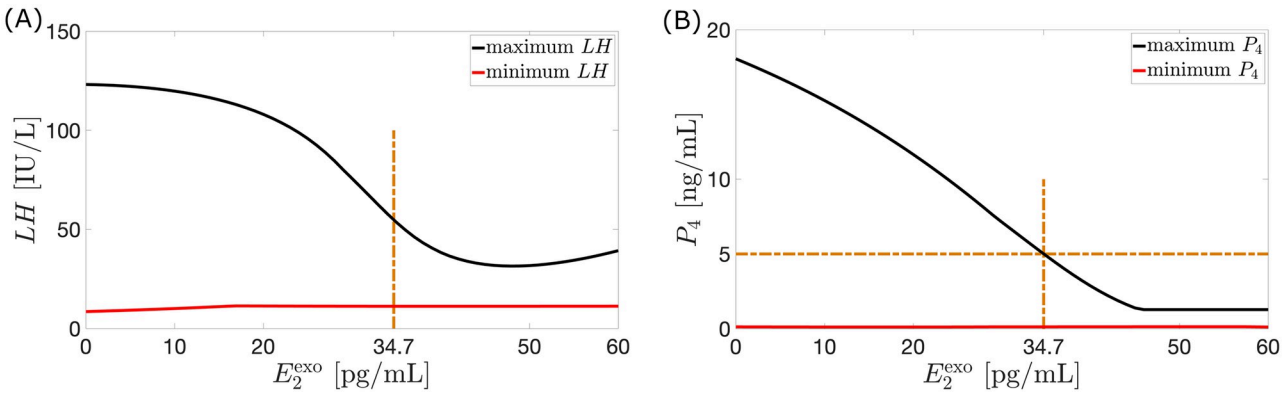

Fig 6. Varying E_2^{exo} dose. The vertical axes in (A) and (B) present the maximum (full black curve) and minimum (full red curve) values over a 28-day cycle reached by LH and P_4, respectively, when the corresponding amount of exogenous E_2 is given. Panel (B) is similar to (A) but shows that increasing dosage of E_2^{exo} causes decreasing amplitude of the variation in P_4 level. Anovulation is attained when $E_2^{exo} > 34.7$ pg/mL.

https://doi.org/10.1371/journal.pcbi.1010073.g006

$E_2^{exo}(t)$, and 0 to 4 ng/mL per day on a 0.1 ng/mL-interval for $P_4^{exo}(t)$. Figs 6 and 7 illustrate that increasing dosage leads to eliminating LH surge and decreasing fluctuation in P_4 level. In the estrogen monotherapy, higher $E_2^{exo}(t)$ generates lower maximum P_4 and anovulation is attained when $E_2^{exo}(t) > 34.7$ pg/mL. In progesterone monotherapy, ovulation is suppressed between doses 3.1 ng/mL and 3.7 ng/mL. The small window of anovulation is due to $P_4^{exo}(t)$ in Eq (15), and the linear inhibitory terms $P_4(t)/w$ and $P_4(t)/q$ in Eqs (3) and (5). Because the inhibitory term $P_4(t)/w$ is linear, to bring $P_4(t) < 5$ ng/mL the amount of $P_4(t)$ must provide strong inhibition of FSH. This is attained by increasing $P_4^{exo}(t)$ in Eq (15). A high amount of $P_4^{exo}(t)$ also enhances inhibition of the linear term $P_4(t)/q$ on $RcF(t)$, which in turn suppresses further $Lut_3(t)$ and $Lut_4(t)$. However, because of the inclusion of $P_4^{exo}(t)$ in Eq (15), increasing amount of $P_4^{exo}(t)$ also results to raising $P_4(t)$ toward values more than 5 ng/mL, which are ovulatory levels.

As in [13], an anovulatory effect of a high dosage of exogenous estrogen or progesterone can be achieved by using a combination of the two hormones. For instance, monotreatment by $P_4^{exo}(t)$ between 3.1 ng/mL per day and 3.7 ng/mL per day or $E_2^{exo}(t)$ greater than 34.7 pg/mL per day for the entire 28-day cycle induces anovulation (see Figs 6(B) and 7(B)). Fig 8(A)

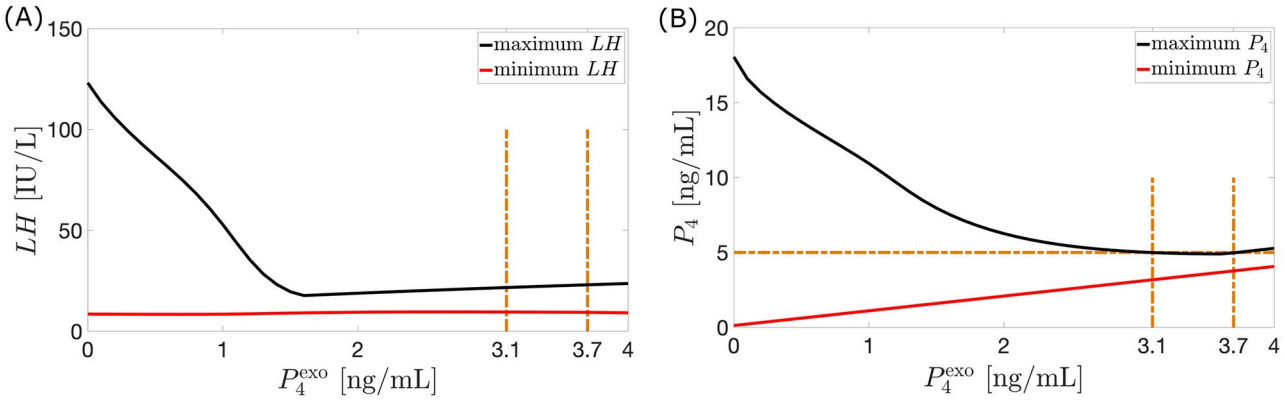

Fig 7. Varying P_4^{exo} dose. Shown in (A) and (B) are the maximum (full black curve) and minimum (full red curve) values attained by LH and P_4 over a 28-day cycle resulting from the administration of the corresponding dosage of P_4^{exo}. Panel (B) illustrates diminishing fluctuation in P_4 value. Anovulation is achieved between $P_4^{exo} = 3.1$ ng/mL and $P_4^{exo} = 3.7$ ng/mL.

https://doi.org/10.1371/journal.pcbi.1010073.g007

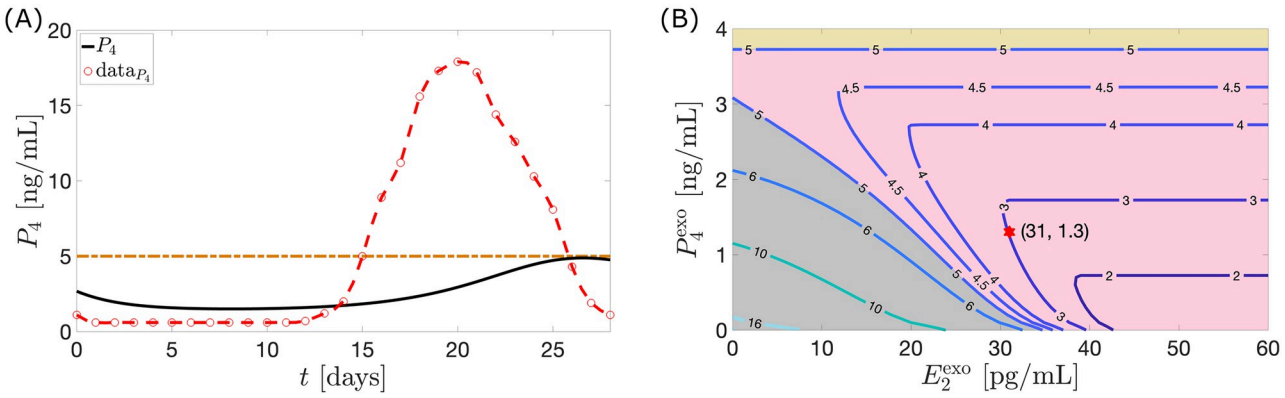

Fig 8. Constant dose combination therapy. (A) The black curve represents the P_4 model output for a combination treatment with $P_4^{exo} = 1.4$ ng/mL per day and $E_2^{exo} = 20$ pg/mL per day administered for 28 days. The red circles with the interpolated curve represents the 28-day normal cycle hormone data extracted from Welt et al. [15]. The treatment suppresses the P_4 concentration achieving anovulatory state. In (B) the curves composed of points (E_2^{exo}, P_4^{exo}), correspond to a combined dosage of E_2^{exo} and P_4^{exo} resulting in a P_4 maximum value of k ng/mL. Anovulation is attained when $k < 5$. The yellow region ($P_4^{exo} > 3.7$ ng/mL) corresponds to ovulation. On the lower left portion, an almost straight line with slope −0.1 separates the regions of ovulation (in gray) and anovulation (in pink).

https://doi.org/10.1371/journal.pcbi.1010073.g008

shows that alternatively, anovulation can be obtained by a combination treatment with $P_4^{exo}(t) = 1.4$ ng/mL per day and $E_2^{exo}(t) = 20$ pg/mL per day. Recall that the monotreatment with $E_2^{exo}(t) = 20$ pg/mL per day or $P_4^{exo}(t) = 1.4$ ng/mL per day does not prevent ovulation (see Fig 5(B)). Other combination treatments which block ovulation are depicted in Fig 8(B).

Fig 8(B) shows contour plots of maximum P_4 levels over a cycle for various combination treatments of $E_2^{exo}(t)$ and $P_4^{exo}(t)$. For instance, the point (31, 1.3) on the contour labeled 3 signifies that an infusion of a combination of $E_2^{exo}(t) = 31$ pg/mL per day and $P_4^{exo}(t) = 1.3$ ng/mL per day yields a maximum P_4 level of 3 ng/mL. The region of anovulation (in pink) is bounded above and on the left by the curves $k = 5$. The left boundary is approximately a straight line with slope −0.1. Thus, to stay on this boundary a reduction of 1 pg/mL per day of $E_2^{exo}(t)$ needs to be counteracted by an increase of approximately 0.1 ng/mL per day of $P_4^{exo}(t)$.

To determine optimal constant dosage resulting in anovulation, P_4 output peaks are recorded for each combination of $E_2^{exo}(t)$ and $P_4^{exo}(t)$ dose. For the estrogen monotherapy, the dosage of E_2^{exo} combined with $P_4^{exo} = 0$ (dosage of P_4^{exo} combined with $E_2^{exo} = 0$ for progesterone monotherapy) resulting in P_4 peak of 4.99 ng/mL is taken as the optimum constant dosage. In the combined therapy, the optimum constant dosage is the nonzero dosage of E_2^{exo} combined with nonzero P_4^{exo} resulting in P_4 peak of 4.99 ng/mL.

Optimal nonconstant dosage

This section uses optimal control to determine optimal time-varying doses that induce anovulation. To explore mono and combination treatments, three different cases of the objective function are examined.

Case 1. **Exogenous estrogen as monotherapy**. Let $u_2(t) = 0$. For $a_1 = 0.4$ μg/mL then the control $u_1(t)$ which minimizes the objective function is illustrated in Fig 9(A).

In Fig 9, the steep rise in the dosage of exogenous estrogen in the optimal control inhibits strongly the release of *FSH* in the bloodstream via Eq (3). This causes the *FSH* levels around the time of u_1 surge to plunge. Consequently, a low mass of *Rc*F (see Fig 10) is produced via Eq (5). The underdeveloped follicles then produce lower E_2, which causes a decrease in *LH* production via Eq (1). Without an *LH* surge, ovulation does not occur. This implies the value of P_4 to be lowered via Eq (14).

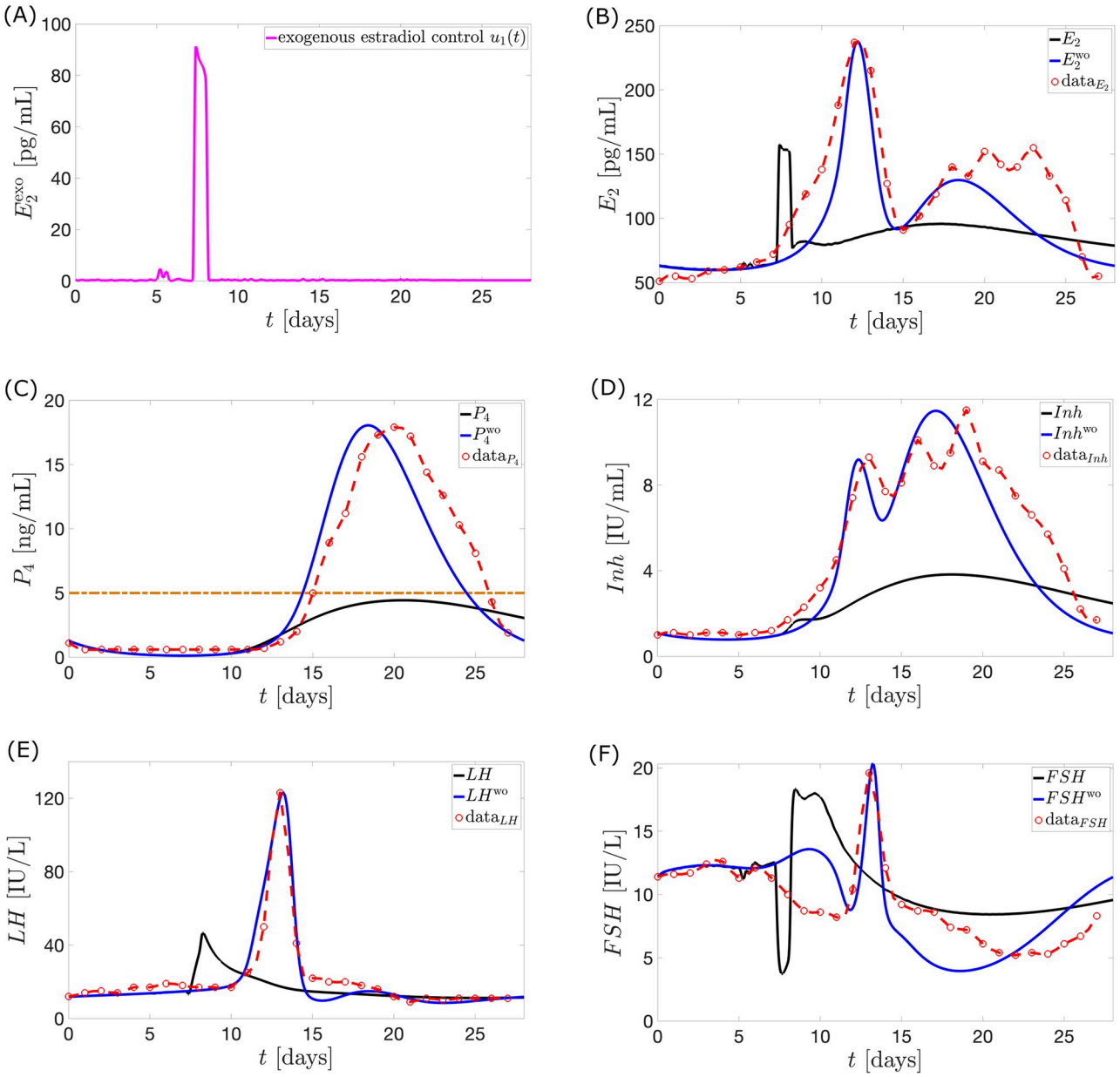

Fig 9. Model output with application of optimal control u_1. The full black curve is the model output when the optimal control u_1 (magenta in panel (A)) is applied. H^{wo} (full blue curve) denotes the hormone model output without the influence of u_1. This is the normal cycle solution. The Welt data for a normal cycle is presented in red circles with the interpolated curve. The maximum P_4 value is 4.43 ng/mL.

https://doi.org/10.1371/journal.pcbi.1010073.g009

The large dosage of $E_2^{exo}(t)$ given in the mid-follicular phase is effective in preventing the ovulatory level of E_2 in the late follicular phase. The schedule of administration agrees with [52] that estrogen treatment started before the 10th day of the menstrual cycle can result in anovulation.

Increasing the value of a_1 penalizes u_1 dose more strongly. This reduces u_1 dose further but increases deviation of P_4 from 4 ng/mL.

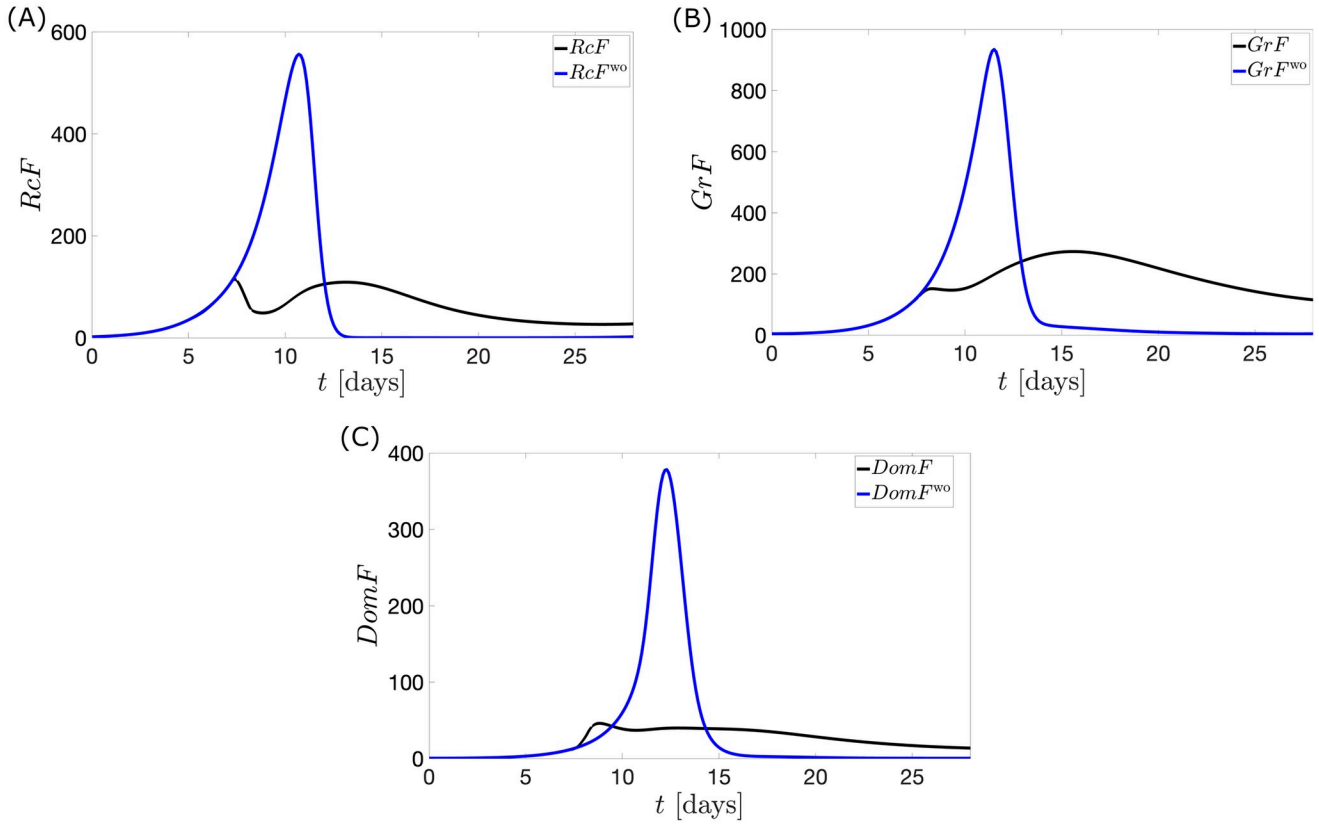

Fig 10. Follicular mass with application of optimal control u_1. The full black curve describes the follicular mass when the optimal control u_1 is applied. The full blue curve shows the follicular mass without the application of u_1. In (A), the steep decline in *RcF* is evident on the interval of *FSH* level drop in Fig 9(F). The inhibition of *RcF* subsequently contributes to the reduced development of *GrF* and *DomF* in panels (B) and (C).

https://doi.org/10.1371/journal.pcbi.1010073.g010

Case 2. **Exogenous progesterone as monotherapy**. Assume $u_1(t) = 0$ and $a_2 = 0.07$ mL^2/ng^2. Anovulatory hormonal levels result from a continuous suppression of *FSH* levels (see Fig 11 (F)), in contrast to the sudden dip in Fig 9(F).

The administration of u_2 starting from the first day of the cycle does not permit *FSH* to reach its maximum value due to the low synthesis in the pituitary via Eq (3). The low level of *FSH* in the follicular phase and the additional inhibition by P_4 via Eq (5) hinder follicular growth. Consequently, E_2 levels far lower than normal are attained via Eq (14). Nonoccurrence of *LH* surge follow via Eq (1).

The optimal control u_2 suggests that a maximum dosage be given before the time in the normal menstrual cycle when P_4 peaks. *Inh* prevents *FSH* synthesis via Eq (3) but anovulation results to decreased *Inh* levels via Eq (16). Thus, the mathematical model causes u_2 to still have high doses after day 14 in order to continue suppression of *FSH* production by compensating for the reduced inhibition by *Inh*.

Similar to Case 1, increasing value of a_2 puts more effort in minimizing u_2 dose, increasing deviation of P_4 from 4 ng/mL.

Case 3. **Administration of combined exogenous estrogen and progesterone**. Allowing $u_1(t) \neq 0$, $u_2(t) \neq 0$, $a_1 = 0.4$ μg/mL and $a_2 = 0.7$ mL^2/ng^2, then the optimal controls u_1 and u_2 illustrated in Fig 12(A) yield the dynamics in Fig 12(B) to 12(F).

The weights attached to the u_1 and u_2 terms result to smaller percentage decrease of u_1 peak from Case 1 compared to the percentage decrease of u_2 peak from Case 2. This leads to a

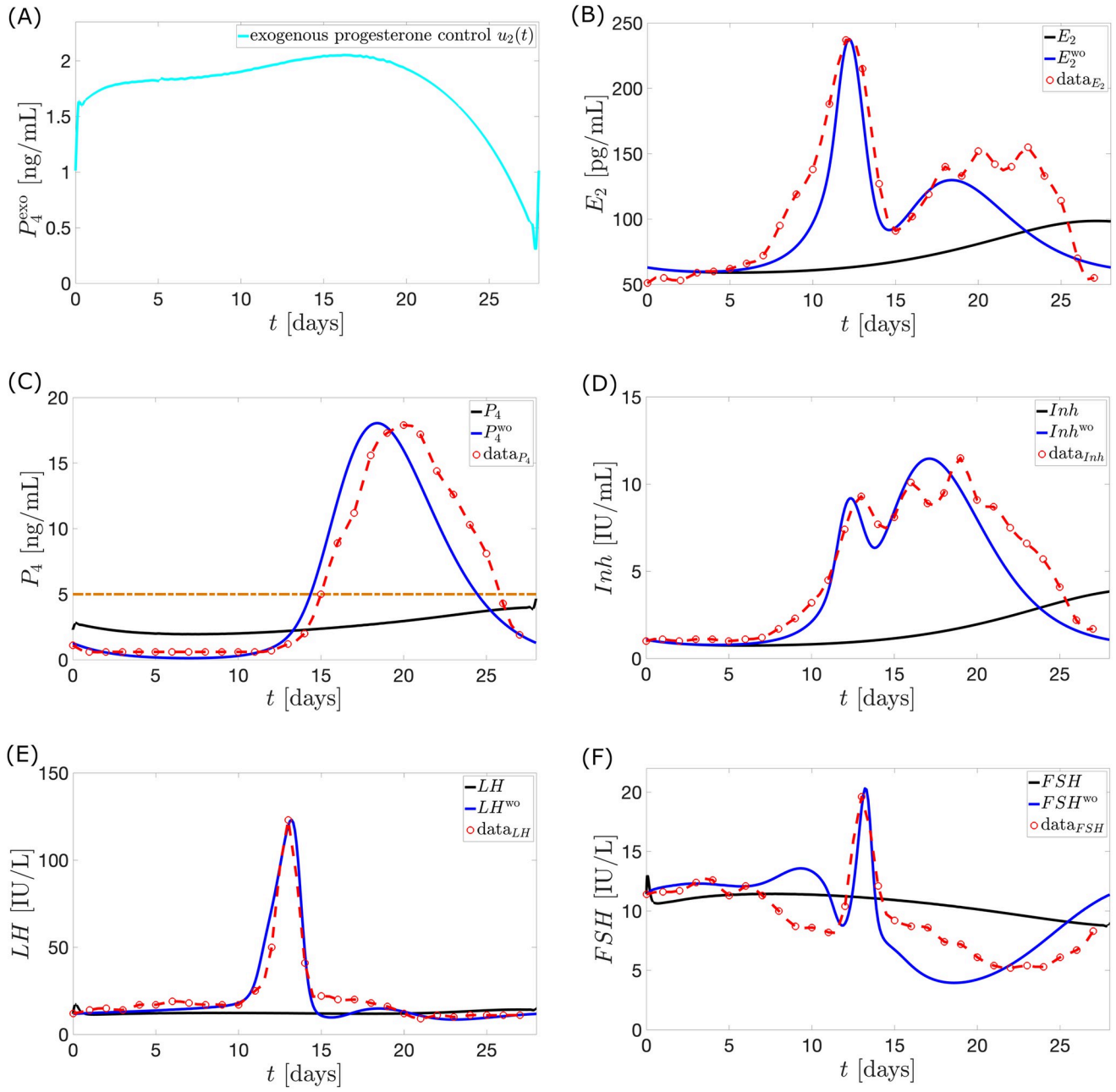

Fig 11. Model output with application of optimal control u_2. The full black curve is the model output when the optimal control u_2 (cyan in panel (A)) is used. The normal cycle solution H^{wo} (full blue curve) is the hormone model output when u_2 is not administered. The red circles with the interpolated curve denote the Welt data for a normal cycle. P_4 reaches a maximum value of approximately 4.66 ng/mL.

https://doi.org/10.1371/journal.pcbi.1010073.g011

greater influence of the optimal control u_1 on the menstrual cycle. Fig 12 presents hormone profiles resembling the ones shown in Fig 9. The weight a_2 may be decreased if the intention is to diminish the impact of E_2.

Not only does the combination therapy utilize lower doses of exogenous estrogen and progesterone, it also allows the administration of u_1 to commence in a later follicular stage. Our simulation shows that the sole administration of estrogen (see Fig 9(A)) blocks ovulation if it is

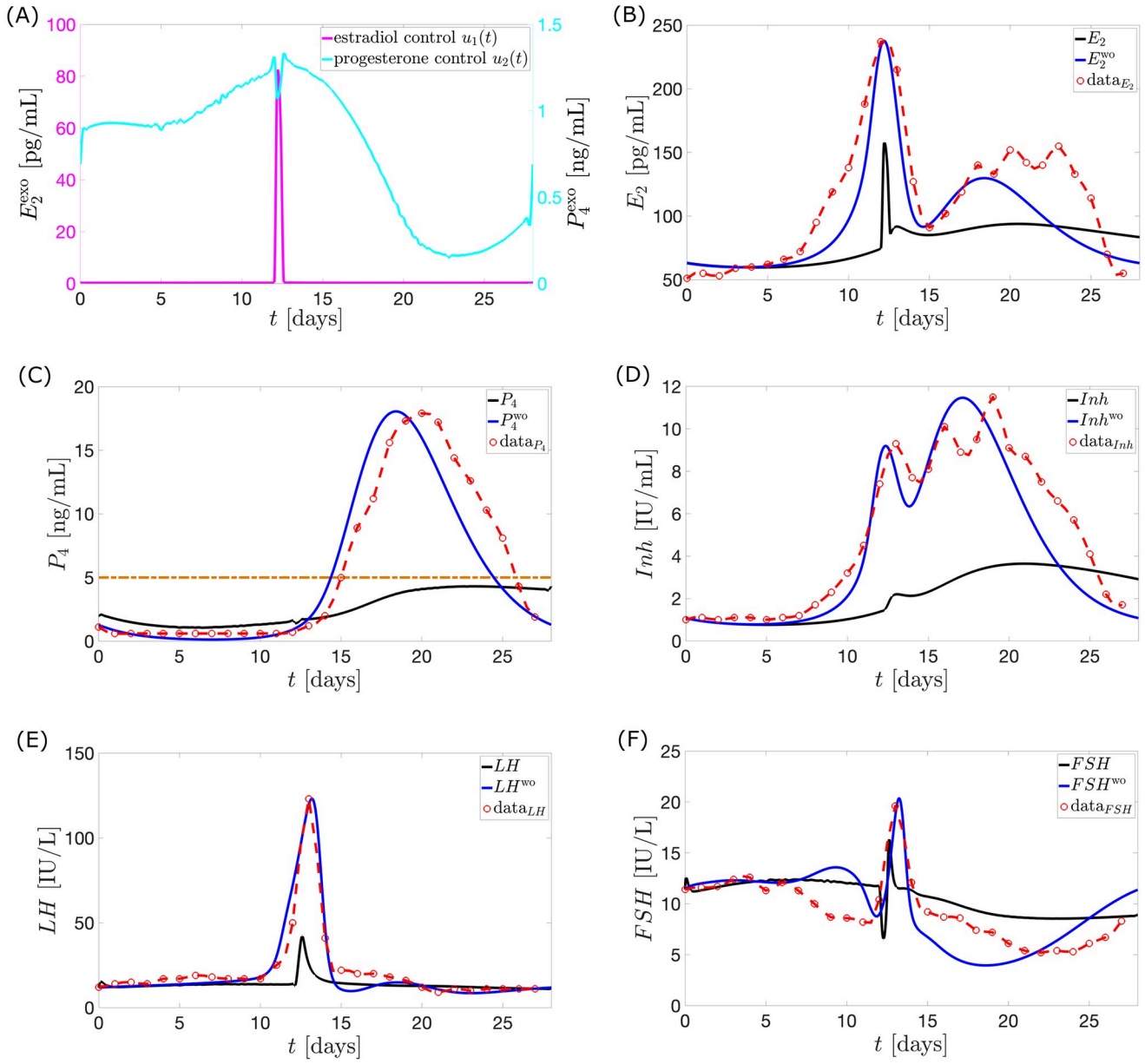

Fig 12. Model output with application of optimal controls u_1 and u_2. The full black curve is the model output when the optimal controls u_1 and u_2 (magenta and cyan in panel (A)) are administered. The normal cycle solution H^{wo} (full blue curve) is the hormone model output when u_1 and u_2 are not applied. The red circles with the interpolated curve denote the Welt data for a normal cycle. The maximum P_4 concentration is approximately 4.31 ng/mL.

https://doi.org/10.1371/journal.pcbi.1010073.g012

done prior to the 10th day of the cycle. Interestingly, the combination therapy (see Fig 12 (A)) suggests that time-varying doses of estrogen and progesterone given simultaneously from the start to the end of the 28-day period, only requires a surge in estrogen dose around the 12th day of the cycle (a delayed administration compared to the estrogen monotherapy). The late administration of u_1 is possibly compensated by the inhibition provided by exogenous P_4 in the early follicular phase. The surge in the u_1 around $t = 12.2$ days allowed a dip in u_2. The combination of the u_1 peak dose and the u_2 dose at this time maintains anovulation. Unlike in Case 1, the dosage and timing of administration of u_1 does not suffice to

keep anovulatory P_4 level until the end of cycle thus, use of increasing u_2 is needed in the late luteal phase.

Discussion

With the rapid development of new implants and injections providing continuous administration there is great potential to implement new treatment scheme minimizing dose. This study employs optimal control to a modification of the model in Margolskee et al. [11] to determine the optimal time-varying dose of exogenous estrogen and/or progesterone that induce anovulation. Biologically, the period length vary within people and between people. This work does not account for this variation, though it can be introduced by varying model parameters or embedding the model in a stochastic framework. This limitation was introduced to generate a simple model that show that contraception can be obtained by manipulating certain parts of the menstrual cycle. The parameter estimation employed yields a model output that predicts the data extracted from Welt et al. [15]. An improvement to previous mathematical models, hormone output peaks are close to the data peaks (see Table 2). This is essential since an anovulatory cycle is determined from the reduction of the normal maximum P_4 level to less than 5 ng/mL and the lack of *LH* surge. The cycle length is also close to the 28-day period of the Welt data. This makes the model beneficial in future studies investigating the effect of exogenous hormones on cycle length.

Exogenous estrogen and/or progesterone inhibits pituitary and ovarian maximum hormone levels [37, 38]. In the model, the administration of exogenous estrogen and/or progesterone caused a reduction in maximum hormonal values (see Fig 5). Such effect is also produced by the hormonal contraception model in Wright et al. [13]. With $E_2^{\text{exo}}(t) = 20$ pg/mL per day, the current model suppresses more the peaks of three of the five hormones but with $P_4^{\text{exo}}(t) = 1.4$ ng/mL per day, the Wright model reduces more the peaks of four of the five hormones (see Table 3). The model in Wright et al. [13] provides greater repression by exogenous P_4 because it uses a nonlinear term to inhibit *RcF* growth and an additional equation depicting upregulation of P_4 by E_2, boosting the contraceptive effect of P_4. We opted for the linear inhibitory term $P_4(t)/q$ and fewer additions to the Margolskee model [11] to keep the current model simple, reducing the computation time in running our optimization code. This is because the numerical method used in this study, control parameterization using MATLAB functions `dde23` and `fmincon`, though easy to implement is not cost effective. Computation time ranges from few hours to several days depending on the proximity of initial guess to the optimal solution. Table D in S1 Text illustrates some examples.

To our knowledge there has been no study applying optimal control theory on the menstrual cycle model. Optimal control could provide drug administration scheme which greatly enhances contraception outcome by significantly minimizing risks associated with high doses such as venous thromboembolism and myocardial infarction [3, 30–32]. The study by Gu et al. [53] showed that compared to constant-dose administration, optimal control results could substantially improve HIV treatment. Results of our work similarly suggest the significant advantage of optimal time-varying doses.

In estrogen monotherapy, the minimum constant dosage of estrogen over 28 days resulting in an anovulation is (34.73 pg/mL) × 28 = 972.44 pg/mL (see Fig 13(A)). This dosage lowers the maximum P_4 level to 4.99 ng/mL. The administration of the optimal control u_1 is able to bring down the maximum P_4 level to 4.43 ng/mL (i.e., anovulation is achieved) with only a total dosage (area under the curve or AUC) of 77.76 pg/mL (see Fig 13(B)). A dosage of 894.68 pg/mL (about 92% of minimum total constant dosage) would be saved if u_1 is used to induce anovulation.

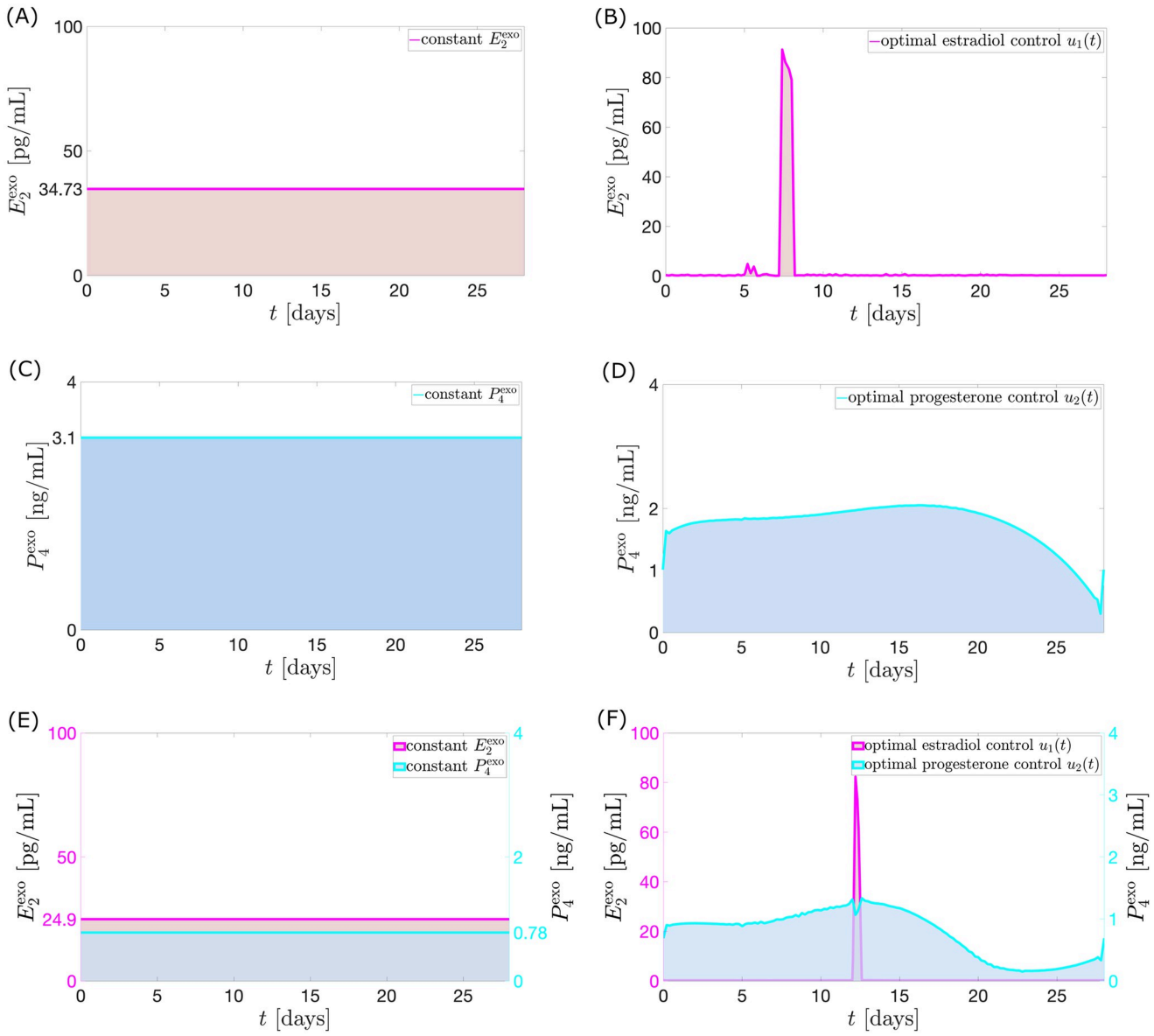

Fig 13. Constant dosage and nonconstant dosage comparison. The shaded regions in Panels (A), (C), and (E) indicate the minimum total constant dosage of exogenous estrogen and/or progesterone over 28 days that lowers maximum P_4 concentration to 4.99 ng/mL. The shaded region below u_1 (area under the curve or AUC) in Panel (B) is the total nonconstant dosage of exogenous E_2 which suppresses the P_4 level to 4.43 ng/mL, a reduction by about 92% of the total dosage in (A). Panel (D) illustrates the total nonconstant dosage of exogenous P_4 that reduces maximum P_4 to 4.66 ng/mL, a reduction by about 43% of the total dosage in (C). Panel (F) shows the combined nonconstant doses of exogenous E_2 and P_4 that gives a maximum P_4 level of 4.31 ng/mL.

https://doi.org/10.1371/journal.pcbi.1010073.g013

A constant intravenous infusion of a low dose of estradiol result in complete shut down of the GnRH pulse generator on female rhesus monkeys for several days or weeks [54, 55]. Although endometrial bleeding is rare in this species, a constant administration may induce a growth of female human endometrium exposing to hyperplasia and bleeding. It justifies the need for an open window without estrogen to allow endometrial bleeding. The optimization result for the time-varying administration of estrogen suggests a dosing regimen generating an estrogen-free window. As is the case with new drug regimen, clinical studies would further

assess the effects of restraining the administration of exogenous estrogen to shorter periods and varying regimens.

In the progesterone monotherapy, u_2 is able to bring down the maximum P_4 level in 28 days to 4.66 ng/mL with only a total dosage (AUC) of 48.84 ng/mL (see Fig 13(D)). A constant administration would require 3.1 ng/mL per day, a total dosage of (3.1 ng/mL) × 28 = 86.8 ng/mL to lower the maximum P_4 to 4.99 ng/mL (see Fig 13(C)). A dosage of 37.96 ng/mL (about 43% of the total dosage for constant administration) would be saved if u_2 is employed.

Exogenous progesterone like progestin may affect the hypothalamo-pituitary ovarian axis differently compared to endogenous progesterone. The current model shows a principle of contraception with exogenous administration of progesterone. If the influence of a specific exogenous progesterone is represented, the current model should be coupled with a pharmacokinetics model that describes the details of the drug.

Now in the combination therapy, the total dosage given by u_1 (AUCu_1) is 35.58 pg/mL while that of u_2 (AUCu_2) is 21.67 ng/mL (see Fig 13(F)). If AUCu_2 is taken and spread out constantly in 28 days, then $P_4^{\text{exo}}(t) = 0.78$ ng/mL (see Fig 13(E)). Consider the least amount of $E_2^{\text{exo}}(t)$ administered constantly in combination with this $P_4^{\text{exo}}(t)$ that results to anovulation. Guided by the contour plot (see Fig 8(B)), $E_2^{\text{exo}}(t) = 24.9$ pg/mL suppresses maximum P_4 to 4.99 ng/mL. The difference between the total exogenous estrogen dosage between the constant and nonconstant administration is (24.9 pg/mL) × 28 − AUCu_1 = 661.62 pg/mL. Hence about 94.89% of the total E_2^{exo} dosage for constant administration would be saved if the combination of u_1 and u_2 is taken. On the other hand, if the total dosage (AUCu_1) given by u_1 is spread out constantly in 28 days, then $E_2^{\text{exo}}(t) = 1.27$ pg/mL. The contour plot (see Fig 8(B)) implies that the least amount of $P_4^{\text{exo}}(t)$ which can be given constantly in combination with $E_2^{\text{exo}}(t)$ to decrease maximum P_4 to 4.99 ng/mL is $P_4^{\text{exo}}(t) = 3$ ng/mL. The difference between the total $P_4^{\text{exo}}(t)$ dosage between the constant and nonconstant administration is (3 ng/mL) × 28 − AUCu_2 = 62.33 ng/mL. Hence about 74.20% of the total P_4^{exo} dosage for constant administration would be saved if the combination of u_1 and u_2 is used to inhibit ovulation. A summary of the results of the optimal control strategies is shown in Table 4.

The optimal control results provide the best timing of administration since an earlier or delayed application of u_1 and/or u_2 yields higher P_4 level. For instance, if the large-dose portion of u_1 is applied in equal intervals from day 35 to day 280 (see Fig 14, anovulation is no longer induced beginning on the 5th 28-day period (i.e. from day 140 to day 280). This is because the application of u_1 in the preceding period changes the dynamics of the menstrual cycle in the succeeding days. One of these changes is the cycle length. Now, because the control u_1 must be administered at a time before E_2 surge (when u_1 is not applied), the timing of administration in the next cycles must also be changed to continuously suppress ovulation. Sometimes resulting cycle length is less than 28 days so only a portion of u_1 will be applied. In addition, because lower levels of u_1 are negligible compared to the higher levels, we applied only the large-dose portion of u_1 from day 35 to day 280 (see Fig 14). The administration is done when E_2 level is increasing and reaches 75 pg/mL. We are currently conducting further investigation to

Table 4. Maximum progesterone level throughout a menstrual cycle caused by the indicated total dose of the optimal exogenous hormone.

Treatment regimen	Total dose	maximum P_4 level
estrogen monotherapy	77.8 pg/mL	4.43 ng/mL
progesterone monotherapy	48.8 ng/mL	4.66 ng/mL
combination therapy	estrogen = 35.6 pg/mL progesterone = 21.7 ng/mL	4.31 ng/mL

https://doi.org/10.1371/journal.pcbi.1010073.t004

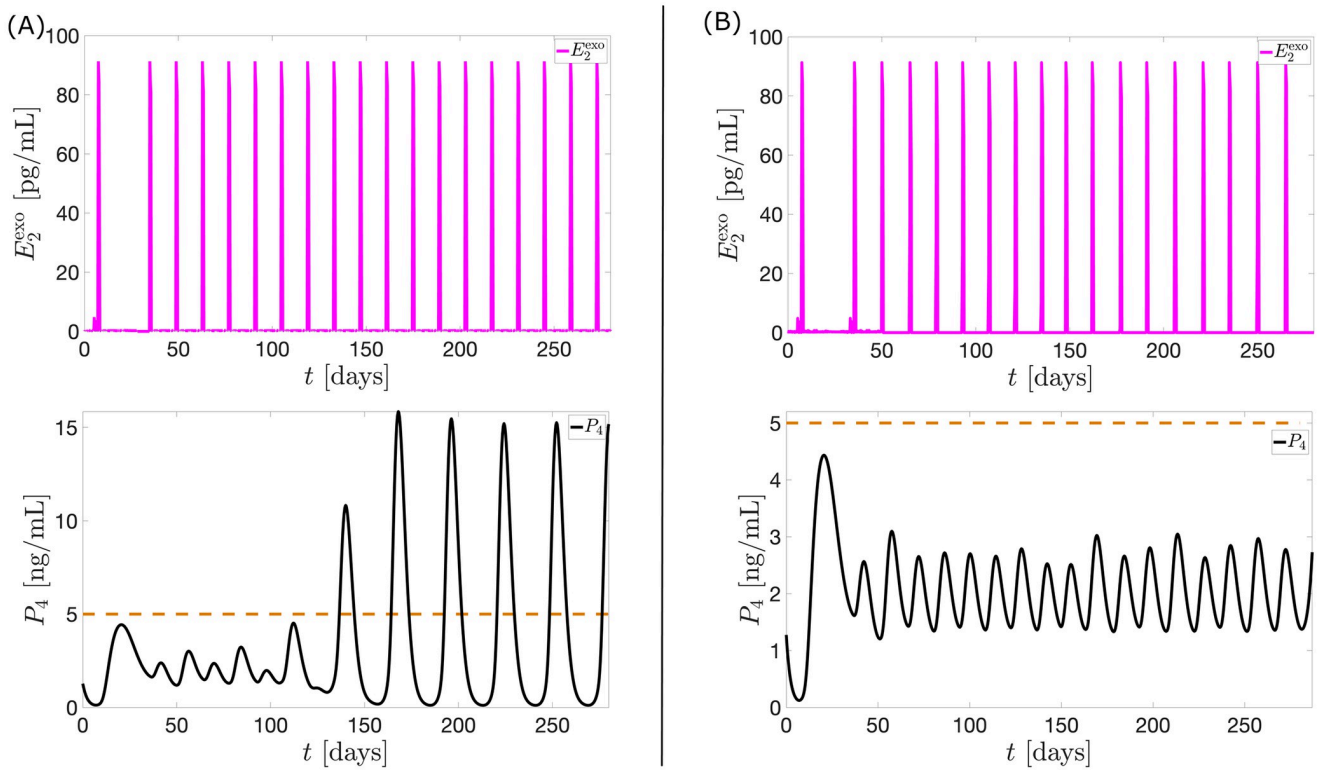

Fig 14. Multiple application of optimal control u_1. The black curve is the model output when multiple u_1 (magenta curve) is applied. In panel (A), the application of u_1 from day 35 to day 280 in equal intervals is unable to sustain anovulation. Panel (B) shows a scheme for administration of multiple u_1 which continuously blocks ovulation.

https://doi.org/10.1371/journal.pcbi.1010073.g014

determine the highest E_2 hormone level where administration of u_1 would commence to still inhibit ovulation. Note that although u_1 is applied eighteen times (in unequal intervals) from day 0 to day 280, the total dosage is still significantly lower than the total constant dosage of exogenous E_2 which induces anovulation. The dosing regimen presented, where administration is triggered by a specific biomarker, here the 75 pg/mL-E_2 level, offers insights on construction of timed devices that give contraception at certain parts of the menstrual cycle. For instance, contraceptive dose may be given relative to E_2 level. This is analogous to the study where *LH* levels are used as indicator for the time of antagonist administration in GnRH antagonist protocols [56]. So even if some patients' cycle length vary a little bit from month to month, their E_2 level can be measured to know when to make a contraceptive device spike.

Result of the sensitivity analysis performed on the model (see Fig A in S1 Text) shows parameters which largely affect model output. To explore adaptability of our control method to different menstrual cycle conditions, we perturb some of the most sensitive parameters to generate model output with different cycle lengths and peaks. Because of its biological significance, we perturbed the third most sensitive parameter km_{LH}. This parameter is the E_2 value at half saturation, it signals strong stimulation in the production of E_2 necessary for ovulation. With km_{LH} equal to 115 pg/mL and 160 pg/mL, we yield model outputs of cycle length 26.92 days and 29.08 days, respectively. Applying the code for optimal nonconstant estrogen monotherapy gives the optimal control u_1 profile in Fig 15(B). The effect of the control in Fig 15(B) on the P_4 level is illustrated in Fig 15(C). These figures show how the optimal control dosage and timing of administration adjust to the varied cycle types.

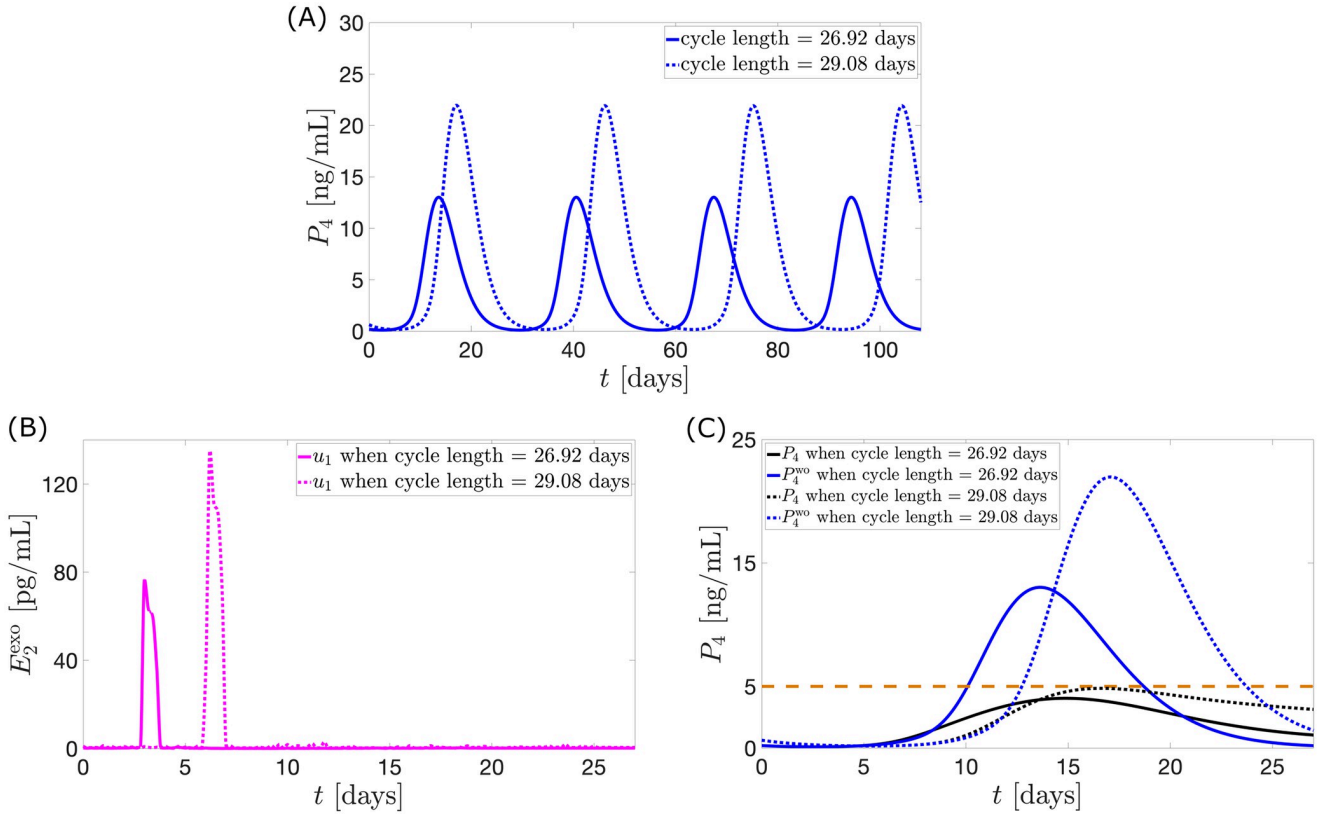

Fig 15. Optimal control u_1 on different cycle lengths. Panel (A) shows model output curves with different cycle lengths. Panel (B) presents the optimal control u_1 obtained by applying the objective function for estrogen monotherapy. The effect of u_1 administration on P_4 peak is described in Panel (C).

https://doi.org/10.1371/journal.pcbi.1010073.g015

The methodology utilized in this study can be adapted to varied cycle conditions as discussed but we recognize some limitations. For instance, several studies have reported that menstrual timing is not precisely known in all women [57–60]. A prior knowledge of the menstrual timing can effectively identify appropriate administration schedule of hormonal contraception. The reproductive function in women is a very complex multiscale dynamical system highly dependent on both endogenous and exogenous hormones thus, the model developed in this study does not capture all factors involved with contraception. Rather, the model serves as a first step in using mathematical modeling to study the transition to a contraceptive state. When more data on individual hormone variations become available, the approach used here can be extended to use these. Another direction is to couple the model with a pharmacokinetics model to obtain patient-specific model to investigate the effects of specific contraceptives on individual menstrual cycle conditions. This provides avenue to examine further the complex multiscale effects of the factors included in silico. While at present, obtaining daily blood profile could be challenging both for financial and practical reasons, this study may motivate future development of advanced methodologies and technologies in data collection.

Conclusion

This study employs a menstrual cycle model which correctly predicts the pituitary and ovarian levels throughout a normal cycle and reflects the decrease in maximum hormone levels caused by exogenous estrogen and/or progesterone. Optimal control results show that a significant reduction in the dosage of exogenous estrogen and/or progesterone may induce anovulation.

Furthermore, combination therapy lower doses even more. Simulations also show the effectivity of the administration of exogenous estrogen in the mid follicular phase.

Through the years, the reduction of exogenous estrogen and progesterone doses in contraceptives is done to decrease risks for adverse effects such as thrombosis and myocardial infarction. With the advent of fully automated hormone-delivery device like the intravaginal prototype device for cattles [61], continuous hormone administration to significantly reduce exogenous hormone dosages in humans is of interest. Hence, results presented in this paper may give clinicians guidance on conducting experiments about optimal treatment regimen causing anovulation. Because the model output cycle length of 28.05 days is a good approximation to the 28-day data cycle length, the model may also be used to explore how treatments change the period of the menstrual cycle. In future studies, researchers should consider stochasticity in the model to investigate within- and between- women's variabilities and couple the current model with a pharmacokinetics model to take into account the exact nature and metabolisms of administered hormones, allowing investigation into effects of specific drugs. Early optimal control results in this study exhibit noticeable oscillations. By several adjustments to the objective function, we were able to smoothen the control. To further lessen fluctuations in the optimization outcome, usage of other numerical techniques like polyhedral active set algorithm or introduction of dynamic equation to the objective function may be explored. Our work suggests a method of obtaining an optimal regimen for administration of exogenous hormone/s over one cycle. In the future when more cost-effective optimization scheme is accessible, one may build on this process to investigate dosing schemes for multiple cycles. Currently, the process applied over one cycle may be repeated for every cycle. It is also possible to use the result over one cycle to continually suppress ovulation over multiple cycles. Additionally, because there is a biomarker for level of hormones like E_2, P_4, and LH, the results presented here give insights on construction of timed devices that give contraception at certain parts of the menstrual cycle.

Supporting information

S1 Text. Supplementary information file. This file presents the data used in our study, model parameters, standard deviation of model parameters, result of the sensitivity analysis performed on the model, effect of various weights on the optimal control results, optimal control results from different forms of the objective function, and computation time and optimal cost for the optimal control simulations.
(PDF)

Acknowledgments

We thank Dr. James F. Selgrade for the discussions which helped in analysis of results and improvement of the manuscript.

Author Contributions

Conceptualization: Aurelio A. de los Reyes V, Johnny T. Ottesen.

Data curation: Brenda Lyn A. Gavina, Aurelio A. de los Reyes V, Johnny T. Ottesen.

Formal analysis: Brenda Lyn A. Gavina, Aurelio A. de los Reyes V, Mette S. Olufsen, Suzanne Lenhart, Johnny T. Ottesen.

Funding acquisition: Aurelio A. de los Reyes V, Suzanne Lenhart.

Investigation: Brenda Lyn A. Gavina, Mette S. Olufsen, Suzanne Lenhart.

Methodology: Brenda Lyn A. Gavina, Aurelio A. de los Reyes V, Mette S. Olufsen, Suzanne Lenhart, Johnny T. Ottesen.

Project administration: Aurelio A. de los Reyes V, Johnny T. Ottesen.

Resources: Johnny T. Ottesen.

Software: Brenda Lyn A. Gavina, Mette S. Olufsen.

Supervision: Aurelio A. de los Reyes V, Mette S. Olufsen, Suzanne Lenhart, Johnny T. Ottesen.

Validation: Brenda Lyn A. Gavina, Aurelio A. de los Reyes V, Mette S. Olufsen, Suzanne Lenhart, Johnny T. Ottesen.

Visualization: Brenda Lyn A. Gavina, Aurelio A. de los Reyes V.

Writing – original draft: Brenda Lyn A. Gavina, Aurelio A. de los Reyes V, Mette S. Olufsen, Suzanne Lenhart, Johnny T. Ottesen.

Writing – review & editing: Brenda Lyn A. Gavina, Aurelio A. de los Reyes V, Mette S. Olufsen, Suzanne Lenhart, Johnny T. Ottesen.

References

1. Trickey R. Women, Hormones and the Menstrual Cycle: Herbal and Medical Solutions from Adolescence to Menopause. St Leonards, NSW, Australia: Allen & Unwin; 1998.
2. Mihm M, Gangooly S, Muttukrishna S. The normal menstrual cycle in women. Anim Reprod Sci. 2011; 124(3):229–236. https://doi.org/10.1016/j.anireprosci.2010.08.030 PMID: 20869180
3. Speroff L, Fritz M. Clinical gynecologic endocrinology and infertility. 8th ed. Philadelphia, PA: Lippincott Williams & Wilkins; 2011.
4. Talaulikar V, Yasmin E. WHO type 1 anovulation: an update on diagnosis, management and implications for long-term health. Obstet Gynecol. 2020; 22(3):178–190. https://doi.org/10.1111/tog.12665
5. Selgrade J, Schlosser P. A model for the production of ovarian hormones during the menstrual cycle. Fields Inst Commun. 1999; 21:429–446.
6. Schlosser P, Selgrade J. A model of gonadotropin regulation during the menstrual cycle in women: qualitative features. Environ Health Perspect. 2000; 108:873–881. https://doi.org/10.2307/3454321 PMID: 11035997
7. Harris L. Differential equation models for the hormonal regulation of the menstrual cycle [Ph.D. thesis]. North Carolina State University; 2002.
8. Clark L, Schlosser P, Selgrade J. Multiple stable periodic solutions in a model for hormonal control of the menstrual cycle. Bull Math BIol. 2003; 65(1):157–173. https://doi.org/10.1006/bulm.2002.0326 PMID: 12597121
9. Pasteur RI. A multiple inhibin model of the human menstrual cycle [Ph.D. thesis]. North Carolina State University; 2008.
10. Selgrade J, Harris L, Pasteur R. A model for hormonal control of the menstrual cycle: Structural consistency but sensitivity with regard to data. J Theor Biol. 2009; 260(4):572–580. https://doi.org/10.1016/j.jtbi.2009.06.017 PMID: 19560471
11. Margolskee A, Selgrade J. Dynamics and bifurcation of a model for hormonal control of the menstrual cycle with inhibin delay. Math Biosci. 2011; 234(2):95–107. https://doi.org/10.1016/j.mbs.2011.09.001 PMID: 21939671
12. Harris L, Selgrade J. Modeling endocrine regulation of the menstrual cycle using delay differential equations. Math Biosci. 2014; 257:11–22. https://doi.org/10.1016/j.mbs.2014.08.011 PMID: 25180928
13. Wright A, F GN, Selgrade J, Olufsen M. Mechanistic model of hormonal contraception. PLOS Comp Biol. 2020; 16(6):1–23. https://doi.org/10.1371/journal.pcbi.1007848 PMID: 32598357
14. McLachlan R, Cohen N, Dahl K, Bremner W, Soules M. Serum inhibin levels during the periovulatory interval in normal women: relationships with sex steroid and gonadotrophin levels. Clin Endocrinol. 1990; 32(1):39–48. https://doi.org/10.1111/j.1365-2265.1990.tb03748.x PMID: 2110047

15. Welt CK, McNicholl D, Taylor A, Hall J. Female reproductive aging is marked by decreased secretion of dimeric inhibin. J Clin Endocrinol Metab. 1999; 84(1):105–111. https://doi.org/10.1210/jcem.84.1.5381 PMID: 9920069

16. Chen C, Ward J. A mathematical model for the human menstrual cycle. Math Med Biol. 2013; 31(1):65–86. https://doi.org/10.1093/imammb/dqs048 PMID: 23329626

17. Reinecke I, Deuflhard P. A complex mathematical model of the human menstrual cycle. J Theor Biol. 2007; 247(2):303–330. https://doi.org/10.1016/j.jtbi.2007.03.011 PMID: 17448501

18. Reinecke I. Mathematical modeling and simulation of the female menstrual cycle [Ph.D. thesis]. Freie Universität Berlin, Germany; 2009.

19. Röblitz S, Stötzel C, Deuflhard P, Jones H, Azulay DO, van der Graaf P, et al. A mathematical model of the human menstrual cycle for the administration of GnRH analogues. J Theor Biol. 2013; 321:8–27. https://doi.org/10.1016/j.jtbi.2012.11.020 PMID: 23206386

20. United Nations. Contraceptive Use by Method 2019. United Nations; 2019.

21. Practice Committee of the American Society for Reproductive Medicine. Hormonal contraception: recent advances and controversies. Fertil Steril. 2008; 90(5, Supplement):S103–S113. https://doi.org/10.1016/j.fertnstert.2008.08.093

22. Guillebaud J. Contraception: your questions answered. 5th ed. Edinburgh, UK: Churchill Livingston; 2009.

23. Hammarbäk S, Ekholm UB, Bäckström T. Spontaneous anovulation causing disappearance of cyclical symptoms in women with the premenstrual syndrome. Acta Endocrinol. 1991; 125(2):132–137.

24. Yonkers K, O'Brien P, Eriksson E. Premenstrual syndrome. The Lancet. 2008; 371(9619):1200–1210. https://doi.org/10.1016/S0140-6736(08)60527-9 PMID: 18395582

25. Herzberg SD, Motu'apuaka ML, Lambert W, Fu R, Brady J, Guise JM. The effect of menstrual cycle and contraceptives on ACL injuries and laxity: a systematic review and meta-analysis. Orthopaedic Journal of Sports Medicine. 2017; 5(7):2325967117718781. https://doi.org/10.1177/2325967117718781 PMID: 28795075

26. Konopka JA, Hsue L, Chang W, Thio T, Dragoo JL. The effect of oral contraceptive hormones on anterior cruciate ligament strength. The American Journal of Sports Medicine. 2020; 48(1):85–92. https://doi.org/10.1177/0363546519887167 PMID: 31765227

27. Wojtys EM, Huston LJ, Boynton MD, Spindler KP, Lindenfeld TN. The effect of the menstrual cycle on anterior cruciate ligament injuries in women as determined byhormone Levels. The American Journal of Sports Medicine. 2002; 30(2):182–188. https://doi.org/10.1177/03635465020300020601 PMID: 11912085

28. Gray AM, Gugala Z, Baillargeon JG. Effects of oral contraceptive use on anterior cruciate ligament injury epidemiology,. Medicine & Science in Sports & Exercise. 2016; 48(4):648–654. https://doi.org/10.1249/MSS.0000000000000806 PMID: 26540261

29. Rahr-Wagner L, Thillemann TM, Mehnert F, Pedersen AB, Lind M. Is the use of oral contraceptives associated with operatively treated anterior cruciate ligament injury?: a case-control study from the Danish Knee Ligament Reconstruction Registry. The American Journal of Sports Medicine. 2014; 42(12):2897–2905. https://doi.org/10.1177/0363546514557240 PMID: 25428957

30. Inman W, Vessey M, Westerholm B, Engelund A. Thromboembolic disease and the steroidal content of oral contraceptives. A report to the Committee on Safety of Drugs. BMJ. 1970; 2(5703):203–209. https://doi.org/10.1136/bmj.2.5703.203 PMID: 5443406

31. Burkman R, Bell C, Serfaty D. The evolution of combined oral contraception: improving the risk-to-benefit ratio. Contraception. 2011; 84(1):19–34. https://doi.org/10.1016/j.contraception.2010.11.004 PMID: 21664507

32. Mann J, Inman W. Oral contraceptives and death from myocardial infarction. BMJ. 1975; 2(5965):245–248. https://doi.org/10.1136/bmj.2.5965.245 PMID: 1169094

33. Shirin A. Optimal control strategies for complex biological systems [Ph.D. thesis]. University of New Mexico; 2019.

34. Cunningham J, Thuijsman F, Peeters R, Viossat Y, Brown J, Gatenby R, et al. Optimal control to reach eco-evolutionary stability in metastatic castrate-resistant prostate cancer. PLOS One. 2020; 15(12):1–24. https://doi.org/10.1371/journal.pone.0243386 PMID: 33290430

35. Azar AT. Control Applications for Biomedical Engineering Systems. Academic Press; 2020.

36. He M, Zhao L, Powell WB. Optimal control of dosage decisions in controlled ovarian hyperstimulation. Annals of Operations Research. 2010; 178(1):223–245. https://doi.org/10.1007/s10479-009-0563-y

37. Obruca A, Korver T, Huber J, Killick S, Landgren BM, Struijs M. Ovarian function during and after treatment with the new progestagen Org 30659. Fertil steril. 2001; 76(1):108–115. https://doi.org/10.1016/S0015-0282(01)01824-6 PMID: 11438328

38. Deb S, Campbell B, Pincott-Allen C, Clewes J, Cumberpatch G, Raine-Fenning N. Quantifying effect of combined oral contraceptive pill on functional ovarian reserve as measured by serum anti-müllerian hormone and small antral follicle count using three-dimensional ultrasound. Ultrasound Obstetr Gynecol. 2012; 39(5):574–580. https://doi.org/10.1002/uog.10114 PMID: 21997961

39. Wathen N, Perry L, Lilford R, Chard T. Interpretation of single progesterone measurement in diagnosis of anovulation and defective luteal phase: observations on analysis of the normal range. BMJ. 1984; 288(6410):7–9. https://doi.org/10.1136/bmj.288.6410.7 PMID: 6418326

40. BioCycle Study Group. Effect of daily fiber intake on reproductive function: the BioCycle study. Am J Clin Nutr. 2009; 90(4):1061–1069. https://doi.org/10.3945/ajcn.2009.27990

41. Rivera R, Yacobson I, Grimes D. The mechanism of action of hormonal contraceptives and intrauterine contraceptive devices. AJOG. 1999; 181(5):1263–1269. https://doi.org/10.1016/S0002-9378(99)70120-1 PMID: 10561657

42. Kimble T, Thurman A, Schwartz J. Currently available combined oral contraception. Expert Rev Obstet Gynecol. 2011; 6(5):525–538. https://doi.org/10.1586/eog.11.48

43. Baird D, Bäckström T, McNeilly A, Smith S, Wathen C. Effect of enucleation of the corpus luteum at different stages of the luteal phase of the human menstrual cycle on subsequent follicular development. Reproduction. 1984; 70(2):615–624. https://doi.org/10.1530/jrf.0.0700615 PMID: 6422035

44. Sech L, Mishell DJ. Oral steroid contraception. Women's Health. 2015; 11(6):743–748. https://doi.org/10.2217/whe.15.82 PMID: 26673988

45. Bormann I. DigitizeIt; 2021. ver. 2.5. Available from: https://www.digitizeit.xyz/.

46. Setty S, Mills T. The effects of progesterone on follicular growth in the rabbit ovary. Biol Reprod. 1987; 36(5):1247–1252. https://doi.org/10.1095/biolreprod36.5.1247 PMID: 3113504

47. Batra S, Miller W. Progesterone inhibits basal production of follicle-stimulating hormone in ovine pituitary cell culture. Endocrinology. 1985; 117(6):2443–2448. https://doi.org/10.1210/endo-117-6-2443 PMID: 3933964

48. Lin Q, Loxton R, Teo L. The control parameterization method for nonlinear optimal control: a survey. J Ind Manag Optim. 2014; 10(1):275–309. https://doi.org/10.3934/jimo.2014.10.275

49. Lenhart S, Workman J. Optimal control applied to biological models. New York, NY: Chapman and Hall/CRC; 2007.

50. Lewis FL, Vrabie D, Syrmos VL. Optimal control. 3rd ed. John Wiley & Sons; 2012.

51. Digirolamo C. Applications of GPOPS-II to optimal control problems with delays [Ph.D. thesis]. North Carolina State University; 2020.

52. Østergaard E, Starup J. Occurrence and function of corpora lutea during different forms of oral contraception. Acta Endocrinol. 1968; 57(3):386–394. PMID: 5694273

53. Weiqing G, Helen M. Optimal therapy regimen for treatment-resistant mutations of HIV. Contemp Math. 2006; 410:139–152.

54. Ordög T, Knobil E. Estradiol and the inhibition of hypothalamic gonadotropin-releasing hormone pulse generator activity in the rhesus monkey. Proceedings of the National Academy of Sciences. 1995; 92(13):5813–5816. https://doi.org/10.1073/pnas.92.13.5813 PMID: 7597033

55. O'Byrne K, Knobil E. Electrophysiological approaches to gonadotrophin releasing hormone pulse generator activity in the rhesus monkey. Human Reproduction. 1993; 8(suppl_2):37–40. https://doi.org/10.1093/humrep/8.suppl_2.37 PMID: 8276966

56. Liu M, Liu S, Li L, Wang P, Li H, Li Y. LH levels may be used as an indicator for the time of antagonist administration in GnRH antagonist protocols—a proof-of-concept study. Frontiers in Endocrinology. 2019; 10. https://doi.org/10.3389/fendo.2019.00067 PMID: 30809195

57. Ferreira-Poblete A. The probability of conception on different days of the cycle with respect to ovulation: an overview. Advances in Contraception. 1997; 13:83–95. https://doi.org/10.1023/A:1006527232605 PMID: 9288325

58. Royston P. Identifying the fertile phase of the human menstrual cycle. Statistics in Medicine. 1991; 10(2):221–240. https://doi.org/10.1002/sim.4780100207 PMID: 2052801

59. Lynch CD, Jackson LW, Buck Louis GM. Estimation of the day-specific probabilities of conception: current state of the knowledge and the relevance for epidemiological research. Paediatric and Perinatal Epidemiology. 2006; 20(s1):3–12. https://doi.org/10.1111/j.1365-3016.2006.00765.x PMID: 17061968

60. Stirnemann JJ, Samson A, Bernard JP, Thalabard JC. Day-specific probabilities of conception in fertile cycles resulting in spontaneous pregnancies. Human Reproduction. 2013; 28(4):1110–1116. https://doi.org/10.1093/humrep/des449 PMID: 23340057

61. Masello M, Ren Y, Erickson D, Giordano J. An automated controlled-release device for intravaginal hormone delivery. JDS communications. 2020; 1(1):15–20. https://doi.org/10.3168/jdsc.2020-18816 PMID: 36340429